Accepted Manuscript

This is an Accepted Manuscript, which has been through the Royal Society of Chemistry peer review process and has been accepted for publication.

Accepted Manuscripts are published online shortly after acceptance, before technical editing, formatting and proof reading. Using this free service, authors can make their results available to the community, in citable form, before we publish the edited article. We will replace this Accepted Manuscript with the edited and formatted Advance Article as soon as it is available.

You can find more information about Accepted Manuscripts in the Information for Authors.

Green Foundation

1. The origin, characterization and value applications of humins are discussed.
2. De-fossilisation of the chemical industry using carbohydrates as feedstocks will result in strongly increased amounts of humins. Applying Green Chemistry principles, value added applications are beneficial. Many aspects of formation and characterization of humins are currently not well known among the wider audience
3. Process conditions will be optimized to maximize the valorization of humins as part of the overall biorefineries. All major streams of biorefineries including humins will be valorized.

Green Chemistry Accepted Manuscript

avantium

P.O. Box 2915, 1000 CX,
Amsterdam, The Netherlands.   +31 20 586 8080

info@avantium.com
www.avantium.com
C of C: 67111386

Journal Name

ARTICLE

The origin, composition, and applications of industrial humins – a review

Ed de Jong,*[a] Mark Mascal,[b] Sandra Constant,[a] Tom Claessen,[a] Pierluigi Tosi,[a,c] and Alice Mija*[c]

Humins are side-products derived from the acid-catalysed conversion of carbohydrate-containing biomass, including sugars (e.g. glucose, fructose, sucrose), oligosaccharides, polysaccharides, and lignocellulosic feedstocks into hydroxymethylfurfural (HMF), furfural, and levulinic acid. Until recently, humins were primarily burned as a power and heat source, but now several higher value applications for humins are within reach. This review covers the history, state of the art, and future outlook on the subject of industrial humins, including their origin, production conditions, compositions, characterisation, and proposed structures. Current opinion on humins formation mechanisms, kinetic studies, ways to minimise their production, established valorisation routes, and novel applications are also discussed.

KEYWORDS: humins; levulinic acid; furfural; HMF; CMF; FDCA; polyesters; acid-catalysed dehydration; biochar; HTC, carbon, lignin, catalyst supports; materials; thermosets, foams, self-healing materials, binders.

1. Introduction

The growing global population and advancing standards of living require increasing amounts of energy that cannot be satisfied by the current status quo.[1] The generation of energy, fuels, and chemicals from renewable resources as an alternative to fossil resources has become a worldwide priority, and is expected to undergo dramatic growth over the next decades.[2] The focus of research, development, and industrial deployment is on process productivities and optimisation of yields, efficiency, feedstock availability and cost and, of course, on the reduction/valorisation of waste/side streams with the goal of establishing a truly circular economy. If we take into consideration the so called "Earth Overshoot Day,"[3] the index calculated by the Global Footprint Network that measures the date of the year on which humanity has used more natural resources than the Earth can renew in one year (i.e. by overfishing, overharvesting, over-emission of CO_2 into the atmosphere, etc), an impressive trend emerges. Back in 1987, the Overshoot Day fell on December 9th, while in 2024 this day was reached already on August 1st. Therefore, despite the significant ecological improvements gained by using renewable resources over fossil/non-renewable ones, a close look needs to be focused on the reduction of CO_2 emissions and the reduction/valorisation of waste/side-products. This needs to lead to the progressive transition from an unsustainable linear economic model[4] to a sustainable circular one.[5–7] There is some consensus globally on the need to move to a 100% renewable

and decarbonised energy sector, for example by using solar, wind, and hydropower sources. However, there is not yet an equivalent strategy for the materials sector, where carbon is indispensable. This is especially true for the chemical and plastics industries, where progress away from fossil-based carbon feedstocks towards above-ground carbon sources has been slow. Under a renewable carbon strategy for the chemical industry, manufacturers would need to stop using all fossil sources and instead use renewable carbon, such as carbohydrates from plants or atmospheric CO_2, in addition to recycling as much carbon as possible (Fig. 1). Thus, industry has to go beyond using renewable energy. All fossil carbon use will ultimately have to end, as the carbon contained in chemicals and plastics is destined to end up in the atmosphere sooner or later.

The Renewable Carbon Initiative is a recent movement to lead this transition by bringing together stakeholders all along the value chain.[6] Solutions such as poly(ethylene furanoate) (PEF) and biobased poly(ethylene terephthalate) (PET), for example,
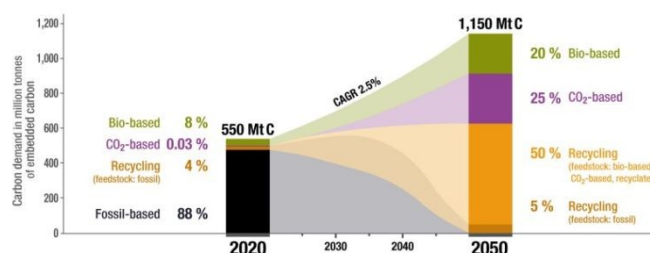
Fig. 1. A possible scenario for world plastic production in 2050 based solely on renewable carbon.[6]

[a] Avantium Renewable Polymers B.V., Zekeringstraat 29, 1014 BV Amsterdam, The Netherlands. Email: ed.dejong@avantium.com

[b] Department of Chemistry, University of California Davis, 1 Shields Avenue, Davis, California 95616, USA

[c] Université Côte d'Azur, Institut de Chimie de Nice, UMR CNRS 7272, 06108 Nice Cedex 02, France. Email: Alice.MIJA@univ-cotedazur.fr

will be crucial for the chemical and plastics industry to initiate the transition from fossil-based resources and embrace the development of sustainable and circular technologies.

Currently, the most widely used renewable resources for chemicals and fuels are starch and sugar-containing crops and to a lesser extent oil crops,[8,9] although both of these raise some issues within the food versus fuel debate.[10,11] In the long run, abundantly available lignocellulosic biomass will be a viable additional resource.[9,12,13] Cellulose, hemicellulose, and lignin are the principal structural components in such biomasses.[14] The polysaccharides can be used as feedstocks for the production of furanic building blocks leading for example to PEF (Scheme 1). Using Brønsted acid-catalysts, polymeric (lignocellulose, starch) or dimeric (sucrose) feedstocks, can be hydrolysed into sugar monomers.[15] Cellulose is hydrolysed to C6-monomers (mainly glucose and some glucose oligomers),[16] while hemicellulose (including xylan, glucuronoxylan, arabinoxylan) is hydrolysed into a mixture of C5 and C6 monomers (including xylose, mannose, and galactose) with relative compositions dependent on the wood source (e.g. hardwoods, softwoods, or grasses).[13,17] Monomeric sugars are then converted into specific derivatives in presence of an acid catalyst with loadings up to 20 mol%.[18,19] The acidic dehydration of C5 sugars results in furfural,[20] while for C6 sugars, the main reaction pathways proceeds through 5-(hydroxymethyl)furfural (HMF)[19,21–27] and levulinic acid (4-oxopentanoic acid, LA)[28,29] with varying selectivities.[15,30–34] Despite extensive investigations into the acid-catalysed dehydration of sugars into

HMF, no consensus on the exact reaction mechanism has been reached.[19,21,35,36] The conversion of glucose into HMF is a multistep reaction, with the first step consisting of a kinetically promoted isomerisation into the more reactive ketohexose fructose.[37] Under acidic conditions, fructose then undergoes dehydration to HMF, levulinic acid (LA) and formic acid.[38,39] The latter acids are formed through rehydration of the C2 and C3 positions of the HMF ring. Historically, levulinic acid was first prepared from sucrose by Mulder.[40] LA, a keto-acid, is stable under most processing conditions and has therefore attracted a lot of interest as platform molecule for a range of products and applications.[34,41–47]

HMF was first reported in 1895 and has found applications as a platform for chemicals as well as fuels.[19] HMF can be converted into a plethora of compounds, such as alkoxymethylfurfurals, 5-(hydroxymethyl)furoic acid, 2,5-furandicarboxylic acid (FDCA), dimethylfuran, levulinic acid, and adipic acid (Scheme 2). These chemicals have applications across a wide range of fields including biofuels, polymers (polyesters, polyamides, polyurethanes), industrial chemicals, pharmaceuticals, and solvents.[15,30–34] For instance, FDCA can replace terephthalic acid as building block for polyesters (PEF and other (co-)polymers).[49,50] To produce the polyester PEF, FDCA is co-polymerised with biobased ethylene glycol derived directly from sugars[51] or via ethanol. PEF is, in many aspects, a technically and environmentally superior polyester to PET.[52,53] [54] This was recently confirmed by an ISO-certified LCA.[53] Currently, the company Avantium is starting up the first FDCA plant in the Netherlands. This flagship plant will allow further deployment of all of the different FDCA applications under development.[53] However, FDCA production is one of many applications of HMF (Scheme 2). Due to the strong interest in the aforementioned products, several feedstocks have been examined for the production of HMF and LA.[55,56] The acid-catalysed dehydration of carbohydrate solutions is however always accompanied by the formation of side-products, and among these the most prominent is a dark-coloured material of low solubility: the so-called humins fraction.[57]
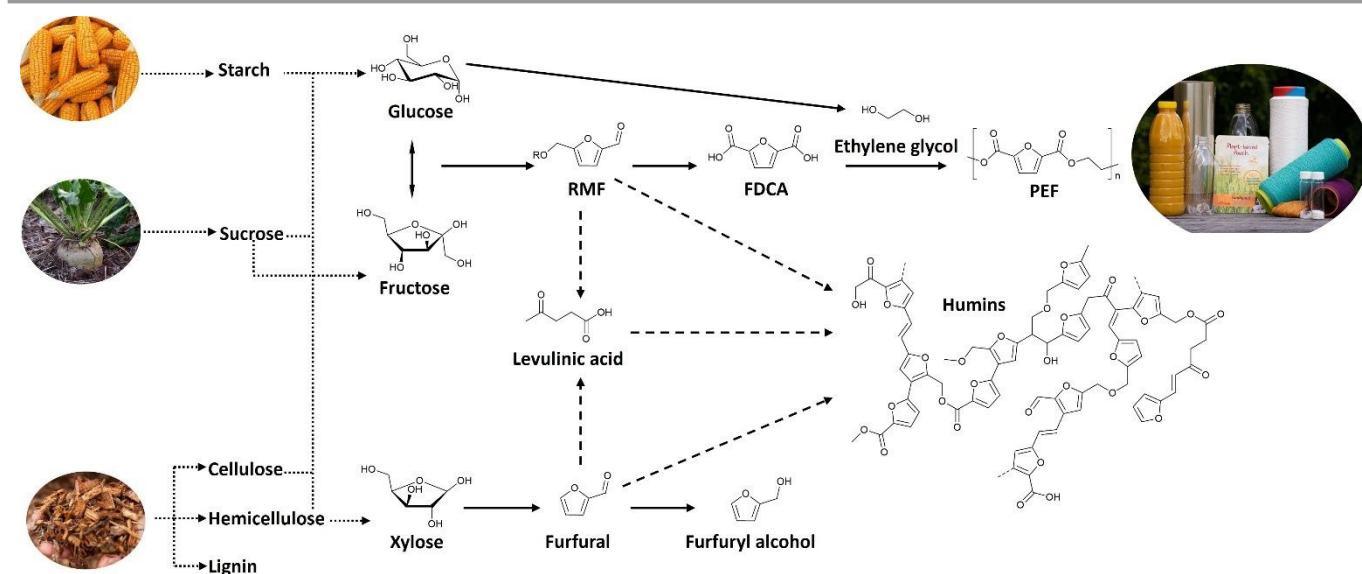
Scheme 1. Different scenarios for the production of furan building blocks from carbohydrates (starch, sucrose, and lignocellulosic biomass). PEF and furfuryl alcohol are two of the potential end products for this class of compounds. Humins are the major side-products in the formation of furanic building blocks.[48]

ARTICLE
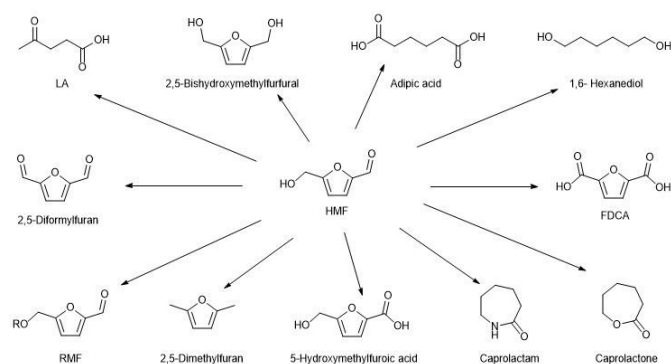
Scheme 2. Molecules derived from HMF, adapted from van Putten *et al.*[19]

Humins production is responsible for the loss of yield in the primary products (HMF, furfural, LA), leading also to engineering challenges (solids handling) and reactor design concerns.[58] As a response to these issues, an alternative to the HMF platform has been developed in the form of 5-(chloromethyl)furfural (CMF).[59,60] Whereas HMF is only practically produced with high yield directly from fructose, and generation from cellulose leads to significant diversion to humic products, CMF can be produced with high efficiency directly from raw biomass. CMF is the main product of the Origin Materials technology,[61] which is now under commercial development using a biomass feed that is not competitive with food production. Also Avantium has recently developed a modified Bergius process in which carbohydrates and polycotton textiles are treated with concentrated HCl to give furanics, especially CMF, without any prior fractionation.[62–65] CMF can be used as a platform molecule in its own right, or converted in high yield to HMF.[66] Although CMF represents a major improvement over HMF, the CMF process is still prone to humins formation. A recent comparative analysis of HMF and CMF production has been published by Karimi and co-workers.[67]

The term humins was firstly used by Muller in 1849 to describe the solid material found during the acid-catalysed dehydration of sucrose.[40] In 1880, Grote and Tollens mentioned the formation of humins as the "dark-coloured caramel" side-product of LA preparation.[68,69] Schweizer[70,71] further characterised humins using various oxidation and halogenation reactions, concluding that humins are a polymerised dehydration product of carbohydrates containing an intact hexose framework, while Blanksma and Egmond[72] were the first to show that humins could be produced directly from HMF.[72] The same term has been subsequently used to also describe humin-like substances,[73] humic solids,[74–76] and in some cases the char that results from the Biofine process for making LA.[15,77] Hayes and co-authors[78] described humin as the insoluble component of soil organic matter that remains after extraction of the other components with aqueous base. Humin usually makes up a substantial component of soil, but its lack of solubility and intractable nature have made it difficult to study. The major components of soil humin are predominantly functionalised aliphatic hydrocarbons, particularly those found in lipids, waxes, cuticular materials, cutin/cutan, and suberin/suberan, which are relatively minor components of

plants. There is also evidence for small amounts of carbohydrates, peptides, and peptidoglycans.[10] However, the role of lignin as a precursor to humins is still under debate.[78,79] Despite the similarity of the terms, it can be concluded that there is little chemical resemblance between the humin found in soil organic matter and industrial humins formed during the acid-catalysed dehydration of carbohydrates.[78]

The structural elements of carbohydrate-derived humins have still not been fully elucidated and remain under active investigation. Humins appear as a complex heterogeneous and polydisperse mixture of oligomers and macromolecules mainly consisting of a furanic network linked by aliphatic chains bearing several oxygen-based moieties (Fig. 2). The elemental composition of acid-catalysed dehydration-derived humins is typically found to be in the order of 55-65% carbon, 4-5% hydrogen, and 30-40% oxygen.[80–84]

Importantly, the humins structure and yields from acid-catalysed dehydration of carbohydrates can vary depending on several factors (e.g. temperature, catalyst, solvent, feedstock, concentrations, residence time). In the earliest studies, humins yields were often not reported by the authors. According to Weingarten et al.,[91,92] humins yields during acid-catalysed carbohydrate dehydration are generally in the range of 8 to 20 mol% starting from HMF, 16-36 mol% starting from fructose, and higher than 32 wt% starting from glucose. Thus, humins formation substantially decreases the selectivity of acid-catalysed dehydration processes. According to economic studies of biobased chemical and biofuel production, the key parameter for improving the economic value of these kinds of conversions is an increase in process selectivity, ideally by avoiding humins formation.[93,94] Unfortunately, the generation of humins has thus far been unavoidable, particularly at industrial scales using relevant feedstock concentrations. Alternatively, humins could be considered a co-product instead of a waste stream and commercially valorised, thereby increasing the economic viability of acid-catalysed sugar dehydration processes.[95,96] However, this scenario requires insights into the molecular structure of humins, their formation mechanisms, chemical behaviour, and reactivity. Here, we review the state of the art in these key knowledge areas to derive a better understanding of humins formation and the development of valorisation approaches.

Table 1. Overview of different humins in relation to production conditions, composition, properties. Humins formed from sucrose in foods have not been extensively characterised up to now. Hardwoods result in more furfural production when woody biomass is used.

Target Product of Process	Companies involved	Intermediate(s) present during humins formation$	Solvent	Feedstock	Lignin present in humins	Appearance (viscosity)	Degree of condensation	Ref.
FDCA	Avantium Renewable Polymers	MMF / HMF / LA / methyl levulinate	Methanol	Fructose	No	Highly viscous	Medium	53
HMF	Michelin/Resicare, Sugar Energy	HMF	Water	Fructose	No	Solid	High	19,85
Purified Terephthalic Acid	Origin Materials	CMF / furfural	Organic solvent / 32% HCl-H_2O	Woody biomass	Yes	Solid	Very high	60
Furoate esters	xF Technologies	HMF / CMF	CH_2Cl_2 / 32% HCl-H_2O	Fructose	No	Solid (5 to 10 nm)	Medium / high	86
Furfural	Many	HMF	Water	Corn cobs, bagasse, hardwood	Yes	Solid	High	87,88
Levulinic acid	GF Bio-chemicals	HMF / furfural	Water	Woody biomass	Yes	Solid	Very high	15,77,89
Caramel	Many	HMF / furfural	None	Sucrose	No	Highly viscous	Very low	40,68,89,90
Balsamic vinegar	Many	AMF / HMF	Acetic acid	Sucrose	No	Viscous	Low	19

$ Intermediates formed include MMF (methoxymethylfurfural); CMF (chloromethylfurfural); AMF (acetoxymethylfurfural)

2. Humins formation in relation to the processing conditions

In general, humins are generated as condensation by-products during the acid-catalysed dehydration of sugars into HMF, furfural, and levulinic acid (Table 1).[80,84,97,98] However, humins can be also produced through other reactions involving carbohydrates, such as the conversion of glucose to ethylene and propylene glycols[99,100] or the conversion of cellulose into ethanol.[101] Also, depending on the operational parameters used during the acid-catalysed dehydration process, humins can present different degrees of condensation and compositions which have a direct effect on their physical characteristics and chemical properties.
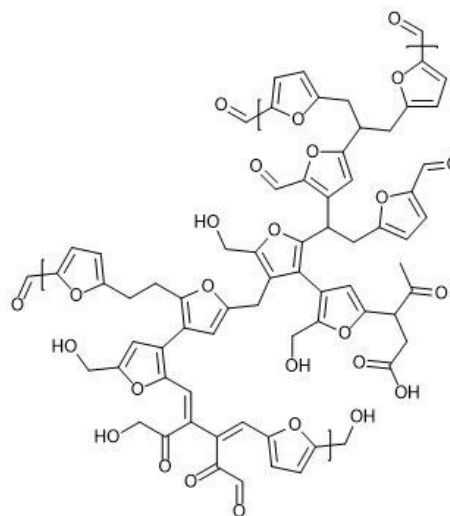

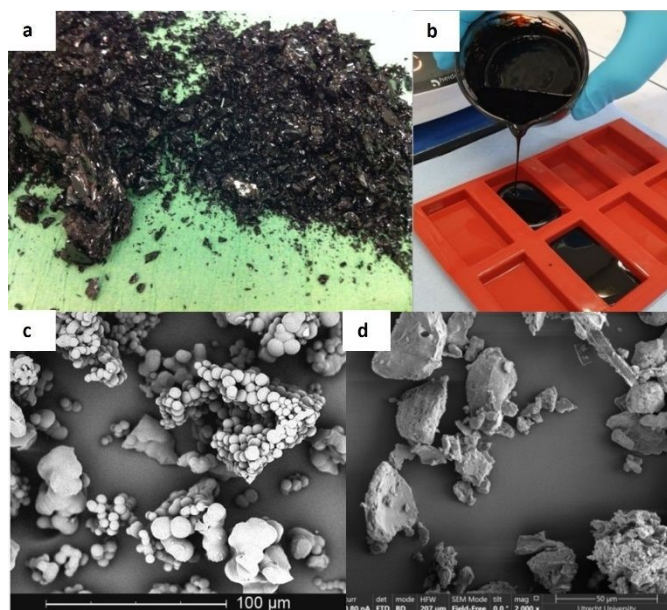Fig 2. A proposed chemical structure for a synthetic, glucose-derived model humin material.[102]

ARTICLE

Fig. 3. Picture and SEM image of highly cross-linked solid humins[103] (a[95] and c), picture of an oligomeric viscous humins [104](b) and SEM image of a dried, water insoluble fraction from viscous humins[48] (d).

Thus, depending on the reaction conditions under which they are produced, humins can appear as solid materials[103,105] or highly viscous liquids.[58,106,107] Severe reaction conditions involving higher temperatures, longer reaction times, higher acidity, and higher feedstock concentrations tend to increase the degree of cross-linking, delivering solid materials usually consisting of agglomerates of spherical particles with a wide size distribution (Fig. 3a and 3c).[103,108] On the other hand, humins derived from milder reaction conditions have a lower degree of cross-linking and are mostly composed of a mixture of oligomers with a broad molecular weight range. The degrees of condensation of humins are also directly correlated with other properties such as solubility, reactivity, and valorisation potential. For instance, solid humins show extremely limited solubility,[109,110] while viscous liquid humins tend to be soluble in organic solvents (Fig. 3b).[48,106] In addition, the higher reactivity and high functional group content of the less cross-linked humins samples allow the development of valorisation pathways through modifications and (co-)polymerisations.[95,96,104,106,107,111–120] Considering the wide variety of humins (Table 1), it is therefore important to refer to the experimental production conditions (feedstock, catalyst, and operating parameters) when comparing studies of humins.

3. Challenges in humins characterisation

Similarly to lignins, humins quantification and characterisation are key elements to estimate their yields, the reaction mechanisms involved, the prevention of their formation, and to develop dedicated valorisation routes. However, humins characterisation presents difficulties due to variations in levels of cross-linking, isolation techniques, solubility properties, yield calculation methods, and differences in feedstock origins. First,

separation of individual humins products and intermediates is difficult to achieve, and often leads to a high degree of fragmentation of the humins, accompanied by a broad range of molecular weights. Also, humins yield determination is not standardized; it is calculated either using the weight of the insoluble material isolated or based on the mass balance of starting material minus the amount of identified monomeric compounds (e.g. HMF, LA, residual carbohydrates). However, the latter calculation method is hampered by assuming a complete dehydration of the furanic moieties, which is often not the case. In addition, the chemical structure of humins is known to vary widely in the nature and number of reactive moieties, and the molecular masses depend on the process used. For example, highly cross-linked humins may undergo aromatisation and various structural rearrangements,[105,121,122] while viscous liquid humins can contain a variety of impurities such as solvents, catalysts, and side products of the biorefinery process, making their actual chemical composition difficult to determine.[58,106] Thus, this lack of rigorous and specific protocols for humins isolation, analysis, and classification leads to challenges in structural understanding and comparisons between humins samples. When lignocellulosic feedstocks are used, the complexity of the humins composition is further increased by the presence of lignin.[15] Unconverted biomass components are incorporated into the humins structure as a cross-linked network. Thus, FT-IR spectra of biorefinery chars clearly indicate the presence of lignin fragments in the humins, while thermogravimetric analysis (TGA) also shows the presence of minor amounts of cellulose and hemicellulose.[15] Recently, humin-lignin hybrids have been characterised by in-depth structural analyses of spruce organosolv lignin isolates, showing the extent to which humin-lignin hybrids form depending on the combined severity applied of the process.[123]

Due to the complexity of humins, characterisation often requires a combination of different approaches including solid and/or solution state analytical techniques (Table 2). Electron microscopy is used to determine the surface morphology of the humins. X-Ray and dynamic light scattering (DLS) allow the estimation of humins particle size and the activation energy of humins formation, both of which lead to better understanding of the humins growth mechanism.[22,124] FT-IR analysis provides insights into the overall structure of humins as well as specific functionalities.[102,125] More detailed structural patterns and functional groups are identified using solid or solution state NMR, depending on the solubility properties of the humins.[48,102,126–128] This compilation of data generates useful insights on humins structure, properties, and formation mechanisms, which will be further discussed in the Section 5. In the following section, we will review how the preparation conditions such as feedstock, catalyst, and solvent can influence the yields and compositions of the resulting humins.

Table 2. Characterisation of humins using different analytical techniques reported in the literature for the three different humins formation systems. Adapted from Liu *et al.*[19]

Humins formation systems	Electron Microscopy	Particle size/ X-ray /light scattering	TGA/DSC	Raman	FT-IR	13C-NMR	1H-NMR	Pyro-GC/LC-MS*
Acid-catalysed dehydration in water	102,103,125,130–132	22,124,133			22,73,102,103, 108,109,125,13 0,133–135	102,136,137	73,97,102,103, 109,137	102,103,130,132,138,139
Acid-catalysed dehydration in organic solvents and bi-phasic systems	48,106,140	141	48,142		48,140,143	48	48,120,126,128 ,144	140,143,145,146
Hydrothermal carbons (HTC)	147–149	147,148,150–152		151,153	153	127,154	154–156	

*Pyro-GC-MS = Pyrolysis Gas Chromatography/Mass Spectrometry.

4. The influence of the experimental conditions on humins formation

4.1. Influence of the process conditions

Acid-catalysed sugar dehydration processes require optimisation, not only in order to maximise the yield of the primary product, but also to reduce the formation of humins.[157–160] The reaction conditions, such as the concentration, temperature, and residence time (often expressed as the so-called "combined severity") have a direct effect on the HMF selectivity and its subsequent conversion into LA. To highlight the strong influence of the temperature, van Putten *et al.*[19] reported that the activation energy of humins formation from HMF is ~100 kJ mol^{-1}, while the HMF rehydration to levulinic acid is in the range 13-110 kJ mol^{-1}.[161] However, these results are in disagreement with kinetic studies performed under milder conditions, in which the selectivity toward levulinic acid relative to the humins pathway shows a weaker dependence on temperature.[108] On the other hand, Girisuta *et al.*[18,81,162] developed kinetic models for humins formation in the acid-catalysed preparation of LA from several feedstocks, showing that humins as side-products cannot be avoided. An activation energy of 164.7 kJ mol^{-1} was calculated for the humins formation,[18] suggesting that milder reaction conditions could potentially limit the generation of these side-products. These observations are in agreement with the kinetic models of Huber *et al.*[158] for LA production, which show that high temperatures and short reaction times (180-200 °C, less than 1 min) maximise the yield of HMF, while lower temperatures and longer reaction times maximise levulinic acid production.[91] In conclusion, longer residence times enhance the rehydration of HMF into levulinic acid along with the concomitant humins formation.[163–165]

4.2. Influence of the catalyst

Combinations of homogeneous and heterogenous catalysts as well as integrated homogeneous-heterogeneous catalytic systems have been investigated in acid-catalysed dehydration reactions of sugars to maximise the HMF and LA yields and limit the formation of humins. However, homogeneous Brønsted acids, such as H_2SO_4 and HCl, are the most commonly used catalysts and currently give the best performance. First, acid concentrations between 3.5 and 10 wt% enhance levulinic acid yields at operating temperatures between 150 and 230 °C.[55] Higher acid concentration and lower reaction temperatures also generally reduce the production of humins, according to kinetic studies.[18,81,91,108,164,166–168] The kinetic model from the Huber group for LA production showed that the process of glucose dehydration to HMF, HMF rehydration into LA, and the simultaneous condensation of intermediates into humins have a first order dependence on the acid concentration.[91] Patil & Lund[108] demonstrated that the acid concentration has a stronger effect on the formation rate of LA than of humins. In other words, higher concentrations of acid catalyst increase the yield and selectivity to LA. Using other Brønsted catalysts such NaHSO$_4$, H$_3$PO$_4$, citric acid, and formic acid at concentrations between 0.016 to 1.6 M at 150 °C, Jung *et al.* showed that the dehydration rate of fructose into HMF and the rehydration rate of HMF into LA do not depend linearly on the acid concentration, but have an exponential dependency.[169] The use of metal chlorides as Lewis acids to facilitate the carbohydrate ring opening[170] and to stabilise of the α-anomer of glucose[171] were also investigated. A kinetic study on the mutarotation of glucose catalysed by Lewis acids was reported Ramesh *et al.*[172] Among the metals tested, the rate of glucose mutarotation follows the order SnCl$_4$ > CrCl$_3$ > AlCl$_3$. CrCl$_3$ was shown to promote isomerisation to the α-glucose anomer. Interestingly, the resulting humins structures also appeared to be different depending on the Lewis acid used. Combined Lewis/Brønsted acid catalysts were studied in xylose conversion to furfural using AlCl$_3$/HCl in water or a biphasic water-methyl isobutyl ketone system in a flow microreactor.[173] A series of parallel and tandem reactions of isomerisation, dehydration, and degradation of xylose were observed, where the Lewis acid catalysed the isomerisation and epimerisation between xylose, lyxose, and xylulose, while both the Lewis and Brønsted acids were active for sugar dehydration to furfural and side reactions leading to humins. The same phenomena were observed using Brønsted-Lewis acidic ionic liquids ([HO$_3$S-(CH$_2$)$_3$-MIM]Cl-FeCl$_3$) as catalysts under hydrothermal conditions.[160]

Heterogeneous catalysts have also been applied to this process. Microporous zeolitic catalysts were investigated, taking advantage of their tuneable properties such as morphology,

Journal Name

ARTICLE

adsorption selectivity, hydrophilic/hydrophobic nature, and acid/base character.[32,163,174] A correlation between the acidity of the catalyst and the enhancement of secondary reactions was observed in that physical deactivation of the catalyst by the humins led to an increased by-product formation rate. Better results were reported using sulfonated chloromethyl polystyrene as catalyst, although further optimisation is still required.[175] Ion-exchange resins have been tested in water in place of the common acids, but the selectivity towards HMF was not improved.[176] Zhang et al.[177] reported a surprisingly high yield of around 94% HMF from glucose in a γ-valerolactone - water solvent using a 50% loading of silicoaluminophosphate zeolite SAPO-34 as the catalyst. However, this could only be achieved at <2% glucose loading. Higher sugar concentrations gave lower yields due to the formation of soluble humins.[148] H-β zeolite $SnCl_2$- phosphotungstic acid/β as a catalyst was also reported, achieving in the best cases yields around 71% of furfural and 30% of HMF in biphasic systems, along with some humins.[178] A direct relationship was observed between reaction time / temperature and the reduction of reaction yields, with an increase of humins and soluble side-products formation. It was reported that, in a catalytic system with the zeolite catalyst H-Beta-25, molecular oxygen could act as both a humins "cleaner" and a reaction accelerator for the synthesis of methyl levulinate (ML) from HMF or furfuryl alcohol (FA).[179] Both the reaction efficiency and the catalyst turnover were significantly improved by the reduction of fouling at the catalyst surface.[179]

Combinations of homogeneous and heterogeneous catalysts have been studied to promote the isomerisation of glucose into fructose and tune the selectivity to HMF and LA. Garcés et al. studied a combination of HCl and β-zeolite catalysts, the latter used for their important contribution of Lewis acidity. An HMF selectivity of 41% from glucose was obtained at 140 °C and 200 ppm HCl for 5 h, whereas more severe conditions were required to reach an LA selectivity of 34% (at 140 °C, 400 ppm HCl, 24 h).[180] A proposed kinetic model, combining the effect of both catalysts, showed a decrease of 30-40% in the activation energy of the main conversion step, along with a reduction in humins yields compared to the previous studies involving only homogenous or heterogeneous catalysts.[150] The presence of NaCl in aqueous reaction systems leads to increased formation of humins.[181] However, Hu et al.[182] showed that both NaCl and cetyltrimethylammonium bromide (CTAB) catalyse the depolymerisation of cellulose and the formation of levulinic acid in a 2-methyltetrahydrofuran/water (MTHF/H_2O) biphasic solvent system. Thus, NaCl promoted humins formation through degradative condensations, whereas CTAB inhibited humins formation by suppressing these pathways, leading to an overall increased LA yield (60.8 mol% from microcrystalline cellulose).[182] Similarly, up to 69.8% HMF yield was obtained from cellulose using hafnyl phosphates as catalysts in a NaCl-H_2O/THF biphasic system.[183] The formation of humins was not avoided, although deposition on the catalyst surface was reduced. Better results were obtained using fructose and glucose as feedstocks, with yields of 94.8% and 90.5% respectively at a 2% substrate loading. The authors suggested that the phosphate groups have a role in the deactivation of

unselective Lewis acid Hf-OH sites that lead to humins. Using a biphasic system (aq NaCl/MIBK) with fructose as feedstock, a highly porous niobium-containing glass matrix with high surface dispersion of niobium oxide showed HMF yields up to 53% with selectivities ranging from 49-65%.[184] Interestingly, no influence of the metal dispersion on the acidity profile was observed. The humin formation correlated with HMF yield regardless of the catalyst employed.[184].

In summary, the promising results obtained with heterogenous catalysts are limited by the deactivation through absorption of the side-products (e.g. humins) on the catalyst surface. Significant challenges in the engineering of economically practical scale-up in these cases will make it difficult to compete with inexpensive homogeneous catalysts such as H_2SO_4 or HCl in the production of HMF or LA from carbohydrates.

4.3. Influence of the solvent

The reaction medium has a strong influence on the efficiency of the acid-catalysed dehydration of sugars. Different systems have been investigated including aqueous, organic, ionic, and bi-phasic media. Water is the most convenient and practical solvent for acid-catalysed dehydration processes. However, low product selectivity and large amounts of insoluble condensed humins are often obtained in this solvent.[103] Currently, polar organic solvents are the most suitable media to solubilise the sugars, stabilise the sugar conformers, and improve catalyst activity. [185] Indeed, water-miscible solvents such as DMSO, ethylene glycol, and other alcohols showed positive effects in the conversion of fructose into HMF compared to the results obtained using water.[164,186,187] These co-solvents influence the reaction kinetics by enhancing HMF formation and slowing its degradation into LA. The humins produced with these solvents are often soluble, which can lead to separation issues alongside other disadvantages.[164] With DMSO, an increased acidity of the medium was observed because of reactive S-containing side-products such H_2SO_4.[186,187] Whitaker et al.[188] showed that DMSO was stable under the reaction conditions (120-150 °C) and that the major acidic species formed were levulinic acid, formic acid, and humins. When alcoholic solvents are used, HMF ethers and levulinic acid esters are formed.[31,53] Ethanol and THF were studied for the synthesis of 5-ethoxymethylfurfural (EMF) from fructose using an SO_3H-substituted cyclodextrin-derived carbon catalyst under ultrasound irradiation.[189] A dependence between selectivity and THF solvent fraction was observed. Using THF it was possible to improve the selectivity for EMF and strongly inhibit humins formation.

To increase the yields and selectivities, already starting in the 1950's, co-solvents in biphasic systems were investigated, such as 1-butanol[190] and methyl isobutyl ketone (MIBK).[138,191–193] These solvents extract the product from the aqueous medium which then limits further condensation reactions to humins. For example, carbon nanotubes in a water/MIBK biphasic system improved the transformation of cellulose into HMF.[194] Deep eutectic solvents (DES) are also promising systems to improve yields.[195,196] They are composed of the quaternary ammonium salt choline chloride (ChCl) and an acid catalyst and form low

melting mixtures with carbohydrates.[197] When ChCl was used in combination with AlCl₃, a 70% yield of HMF was obtained in a water/MIBK system.[198] The selectivity was optimal for a ChCl content of 50 wt% in water. The humins formed in such DES systems were soluble. With a biphasic system consisting of MIBK and a DES composed of ChCl and ethylene glycol (EG), an HMF yield of 63% was obtained from fructose.[199] Gomes *et al.*[21] reported interesting results in the synthesis of HMF from sugars using a biphasic system (aq NaCl/THF) and a combination of Lewis acids (ZnCl₂ and AlCl₃) and a Brønsted acid (HCl). After 1 h reaction time at 180 °C, HMF production was increased using an extraction solvent/reaction solvent ratio ≥ 10. The best HMF yield achieved using glucose as feedstock was 62.7% with ZnCl₂/HCl and 66.9% for AlCl₃/HCl, while the best HMF yield using sucrose was 65.6% using ZnCl₂/HCl and 54.4 % for AlCl₃/HCl.[21] The humins obtained under such conditions were mainly constituted of furanic species, and in particular 2-methylfuran units. When using AlCl₃/HCl, fragments of the humins measured by mass spectrometry were twofold larger than those obtained with ZnCl₂/HCl, showing that catalysts with the stronger acidic nature led to increased oligomerisation and condensation reactions.[21] Another biphasic system, consisting of NaHSO₄/ZrO₂/H₂O-THF showed a maximum HMF yield of 86.5% from glucose.[200] Even though NaHSO₄ was the acid catalyst for HMF conversion, the role of ZrO₂ was to influence the glucose-fructose isomerisation. Humins formation on the ZrO₂ surface could not be avoided, but according to the authors it was sufficiently limited to reuse the catalyst for six additional cycles without reconditioning. Biphasic systems involving isophorone, 2-methyltetrahydrofuran, or cyclopentylmethylether were also tested in the conversion xylose to furfural.[201] The maximum furfural yield was around 78 mol% using cyclopentylmethylether. Again, this study showed that product yields decrease with the increasing reaction time because of humins formation. However, despite the fact that humins formation was not avoided, this is a promising initial investigation given the avoidance of salts. Although several biphasic systems were tested, none was able to strongly reduce humins formation.[31,202] However, interesting results were reported using ternary solvent systems. Fructose dehydration in H₂O/dioxane/MIBK in combination with Amberlyst 70 catalyst gave 93% selectivity and 84% yield of HMF with residence time as short as 1.6 min. The in-situ extraction of HMF from the active aqueous phase to the organic phase by MIBK protected it from unfavourable side reactions and humins formation.[203]

4.4. Influence of the feedstock

The carbohydrate source can also influence the acid-catalysed dehydration yields and the chemical structures of resulting humins. Along with glucose and fructose, other carbohydrate-sources can likewise be converted using acid-catalysed processes.[84] An in-depth study of the conversion of different aldoses and ketoses in both water and methanol showed clear differences in rates, yields, and side-products formed.[25,26] With some sugars, substantial amounts of hydroxyacetylfurfural (HAF) were formed. Velaga *et al.*[141] have reported conversions

of bamboo sawdust, cellulose, glucose, and fructose to LA using mordenite zeolites, achieving 61, 56, 52 and 43% yields, respectively. Similarly, Sievers et al. investigated the hydrolysis and conversion of several lignocellulosics and sugars and, such as pine wood and glucose, fructose, xylose[204] in ionic liquids.[205] They observed that fructose was converted much faster than mannose, glucose, and xylose and yielded HMF with high selectivity. When loblolly pinewood, a lignocellulosic feedstock, was submitted to acid-catalysed hydrolysis, ''pseudo-lignin'' side products (i.e. lignin-humins adducts) were identified.[204] During acid-catalysed dehydration, glucose is partly isomerised into fructose (or at least the intermediate 1,2-enediol), which is kinetically favoured in the dehydration step to HMF.[37,57,206–208] However, glucose is converted into humins at a rate greater than the isomerisation into fructose,[208] which explains the reduction of product yields. Furthermore, it has been reported that HMF production from glucose occurs simultaneously with the apparent formation of water-soluble glucose oligomers, which can release glucose slowly and progressively, thereby acting as glucose "reservoir" for HMF. However, these oligomers can also be incorporated directly in the humins structure.[155] The isomer-dependent conversion rate was confirmed by Kimura *et al.* by ¹³C NMR.[209] As mentioned earlier, the use of Lewis acids in acid-catalysed glucose dehydration leads to increase the isomerisation into fructose and higher HMF yields.[19] In addition, HMF itself plays also a role in the humins generation process. The calculated reaction order for humins formation is 1.3 when fructose is used as feedstock, while it is 1.7 when HMF is used.[131] Sievers *et al.* hypothesized that the humins formation was due to the condensation of several water soluble products with HMF, which is involved in the cross-linked network formation.[204] Therefore, fructose is the best commonly available feedstock to achieve the highest HMF yields.[187] Interestingly, adding LA or glucose to the acid-catalysed dehydration of fructose leads to a decrease in process selectivity and higher amounts of humins are observed according to Tarabanko *et al.*[210] They postulated that the formation of LA in the process is a reaction of first order with respect to substrate concentration, and the humic substance formation is a reaction of second order with respect to the initial carbohydrate loadings. These two process characteristics are the main reasons for decreasing selectivities of carbohydrate conversions at increasing substrate concentrations.[210] Interestingly, Meier *et al.* suggested that the absence of OH groups in position C2 or C5 of pentoses can suppress the formation of humins during the acid-catalysed conversion of such carbohydrates into furanics.[211]

The elemental composition of humins was shown to vary with feedstock. Humins derived from HMF were composed of 58 wt% carbon while humins derived from glucose contained a higher C content (62 wt%).[82] Humins formed during the production of levulinic acid from HMF were found to contain 61.2 wt% carbon.[80] A higher C content of 65.5 wt% was found in humins derived from fructose treated with phosphoric acid at high temperature.[212]

Finally, in all process conditions, the importance of the concentration in feedstock should also not be underestimated.

Indeed, when high loadings of fructose were used, a decrease in conversion to LA and higher humins formation were observed starting at 95 °C.[164,213,214] So, while high feedstock concentrations are necessary to develop economic processes, this comes at the cost of substantial diversion to humins.

To conclude, this section shows the practical limits in terms of process optimisation in the acid-catalysed dehydration of carbohydrates. Despite all attempts to eliminate humins, their formation is still currently unavoidable. However, all the experimental conditions discussed in this section have impacts on the nature of the humins, such as structure, degree of condensation, physical state (liquid versus solid), and reactivity. In the next section, in-depth investigations of humins targeted at the elucidation of their mechanisms of formation, molecular structures, functionalities, physico-chemical properties, and reactivity will be reviewed.

5. Humins formation mechanisms

5.1. Mechanistic insights

The complex molecular structure and the mechanism of humins formation have not yet been unequivocally determined, despite several structural proposals and mechanistic studies. The first study on humins structure was published by Mulder in 1840,[40] who prepared humins by acid-catalysed dehydration of sucrose using HCl, whereby an elemental composition of 64-65 wt% C, 5-6 wt% H, 31-32 wt% O was found. Other investigations conducted around 1938 by Schweizer[70,71,89] proposed that sucrose-derived humins were formed by dehydration reactions, while the pyran ring of the sugar remained intact, a claim which is not confirmed in recent work. The self-condensation of HMF to generate humins was suggested by Zeitsch,[88] which was also proposed for the production of char and tar from sugars treated in (sub)critical water.[153,215] However, while the polymerisation of furfural to resins was already well known,[216] the self-condensation pathway for HMF and furfural could be excluded due to the absence of a hydrogen α to the carbonyl group.[217] It is generally considered that humins derived from C6-sugars are generated via condensations between the dehydrated intermediates of the process (HMF or derivatives).[27] Results of the acid-catalysed hydrolysis and dehydration of cellulose using sulfuric acid in ionic liquids showed that humins yield was directly proportional to the HMF concentration, leading to the speculation that humins were formed by condensation between glucose and HMF.[145] A similar conclusion was drawn for xylose-derived humins, suggesting a condensation between xylose and furfural.[88,92,218]

Using density functional theory-based mechanistic studies and microkinetic analysis on glucose Brønsted acid-catalysed dehydration, it was found that humins could result from polymerisation of HMF ether dimers and acetal trimers with glucose dehydration intermediates.[219] The group of Vlachos used ultra-small angle x-ray scattering (USAXS) to investigate the evolution of the size, morphology, volume fraction, and concentration of humins formed during dehydration of fructose to HMF and the subsequent polymerisation of HMF between

80–95 °C in 1 M hydrochloric acid.[124] The apparent activation energy of humins formation is 102 ± 0.4 kJ·mol⁻¹. The trend in the number of particles over time reveals competing processes entailing continuous nucleation leading to increasing polydispersity and finally aggregation and precipitation. The direct observation of the growth of humins indicates that they are formed primarily from HMF rather than fructose.[124] One study surprisingly excluded a role for HMF in humins formation, where instead FA and glucose mono-dehydration products were indicated as main building blocks.[220]

Several proposals have been reported to elucidate the mechanism involved in humins formation in the acid-catalysed dehydration of sugars.[221] The vast majority of research on industrial humins formation and composition has been performed under aqueous conditions and the most relevant insights are described in the following section.

5.2. Humins formation and composition in aqueous systems

A mechanism for the acid-catalysed dehydration of HMF was suggested by Horvat *et al.* in 1985 and is represented in Scheme 3.[97,137] It was suggested that humins are generated by a poorly defined polymerisation reaction starting from the proposed intermediate DHH (2,5-dioxo-6-hydroxyhexanal), formed from the 4,5-addition of water to HMF and subsequent ring opening. The authors were able to identify four other intermediates of the acid-catalysed dehydration of sugars to humins using in situ NMR and ¹³C labelling studies. However, DHH was never isolated and, if it forms, was therefore believed to be subject to rapid polymerisation into humins. Several subsequent studies have also proposed mechanisms of humins formation via the DHH intermediate. Velaga *et al.*[141] also suggested that the humins formation involves DHH. However, this again appears to be speculation based mostly on literature suggestion and was only supported by inconclusive FT-IR analyses of humins produced during the conversion of HMF into LA using mordenite zeolites. Shi *et al.*[121,122] reported a detailed mechanistic proposal for humins formation by hydrothermal degradation of several model compounds, and the formation of DHH was again suggested as one of the intermediates. Therefore, despite the fact that it has never been isolated, DHH is currently considered one of the most likely intermediates in the generation of humins (Scheme 3). The model based on Horvat's observations was an important first step in the understanding of the mechanism of humins formation. Additional work on the chemical structure of humins and the mechanism of their formation from HMF with different amounts of aldol condensation has been reported.[130]

Several propositions for humins structure and formation mechanism have been subsequently developed by the groups of Weckhuysen,[102,103] Lund and Patil,[108,125] and Sumerskii.[73] In the following sections, these different proposals are further discussed. Although these all help to better understand the process, currently none of them can be considered to fully describe humins structure.
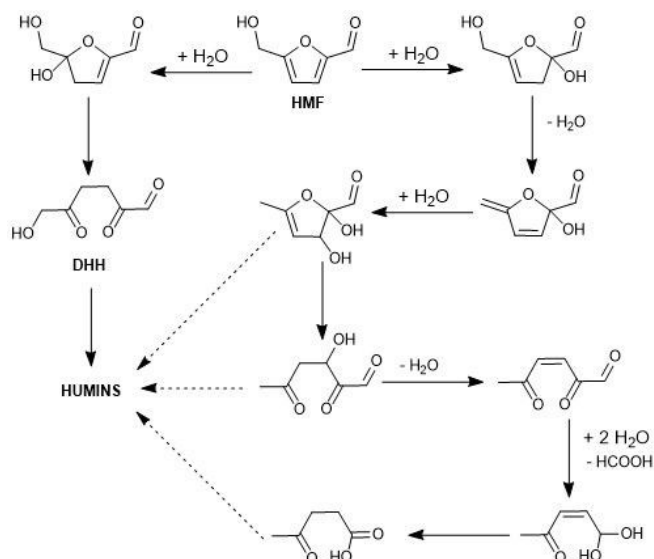
Scheme 3. Humins formation routes from HMF. Redrawn and adapted from Horvat *et al.*[97,137] with permission from Elsevier, copyright 2025.

5.2.1. Mechanistic pathway by Sumerskii and Zerubin group

Sumerskii *et al.*[73] studied humins obtained from reactions in aqueous media with 5 wt% carbohydrates and 0.5% H_2SO_4 at 175-180 °C for 2 h. The solid humins were filtered and the solution was neutralised to precipitate a soluble humins fraction. Roughly 20% of the humins could be extracted with acetone which, according to FT-IR analysis, was associated with an oligomeric fraction. Both the soluble and insoluble humins fractions were characterised. FT-IR spectra revealed the presence of furanic moieties and several oxygen-rich functional groups,[73] in agreement with the ^{13}C NMR analysis of the acetone-soluble fraction. Furanics were also detected by pyrolysis-GC-MS analysis.[73] The authors estimated that the humins structure consisted of around 60% furan rings and 20% of aliphatic linkers. A mechanism for humins formation was subsequently proposed. It involves nucleophilic addition of the hydroxyl group of one HMF molecule to the aldehyde function of another HMF molecule. This step, catalysed by Brønsted acids, generates acetal and hemiacetal bonds which are included in the final humins structure (Scheme 4). Another proposed mechanism involves the protonation of levulinic acid, leading to a species that reacts with HMF via the carbonyl or OH function (Scheme 4).[73] Unlike the mechanism proposed by Horvat, this one does not involve DHH.

5.2.2. Mechanistic pathway proposed by Lund group

Consistent with the mechanism proposed by Horvat *et al.*,[97,137] Lund *et al.*[108,125] suggested aldol addition and condensation as main reaction steps in the acid-catalysed production of humins. These mechanistic hypotheses, as suggested by Horvat, assumed the formation of DHH. Again, the absence of detection of the DHH intermediate was considered as an indication of its high reactivity.[108] Free energy calculations showed that aldol addition reactions were the most favourable of the possible

DHH reactions.[125] They postulated that carbohydrates were first converted into HMF and then DHH in order to form humins. The
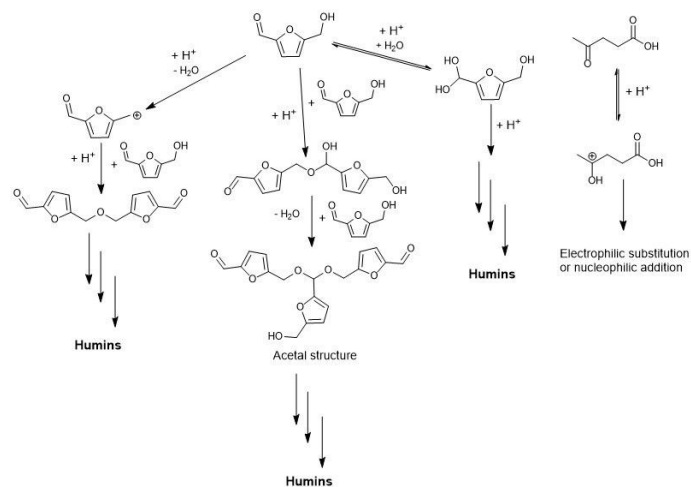
Scheme 4. Humins formation mechanism in water as proposed by Sumerskii et al.[73]
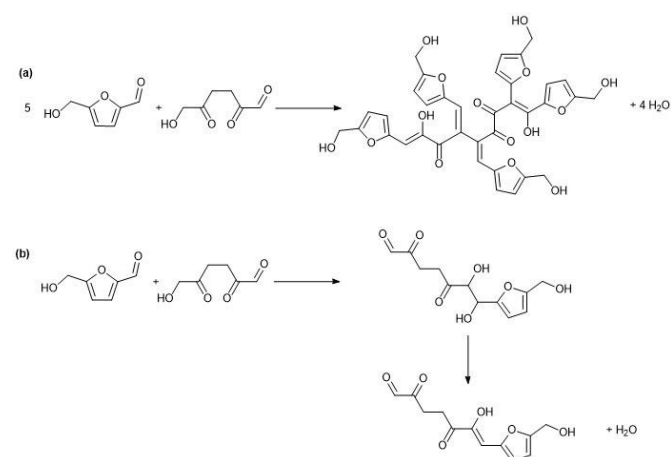
Scheme 5. Two possible processes of humin growth as proposed by Lund *et al.*[108]

authors highlighted two possible processes for humins growth, which are related but mechanistically different (Scheme 5).[108] The FT-IR spectra showed that humins retain the furan ring and the hydroxymethyl group of HMF. Furthermore, benzaldehyde (which does not produce humins under the reaction conditions) can be incorporated in the humins structure if added during the acid-catalysed conversion of HMF. In a later study, FT-IR spectra of humins formed during the acid-catalysed dehydration of HMF, glucose, fructose, and cellobiose were compared.[125] The spectra of products from the acid-catalysed dehydration of glucose and fructose contained two strong peaks at 1625 and 1710 cm^{-1} which were not observed for HMF humins. The authors explained that the higher HMF concentration observed during the reaction resulted in almost exclusive reactivity between DHH and HMF. Furthermore, at high fructose conversion rates, minor accumulation of humins and less incorporation of HMF into the structure was observed, in contrast with the high accumulation of humin products found in glucose or cellobiose dehydration reactions.[125] The

Journal Name

ARTICLE

experimental results showed that the direct formation of humins from glucose, fructose, and cellobiose did not appear to be significant and that the conversion to HMF and then DHH was occurring prior to the formation of the humins. This study supported the hypothesis that humins form during the acid-catalysed dehydration of sugars through aldol additions/condensations. Density functional theory based calculations performed by Velasco et al.[222] The formation of the HMF-DHH dimer was slightly endergonic, while the rehydration of HMF to DHH was thermodynamically downhill.

5.2.3. Mechanistic pathway proposed by van Zandvoort and Weckhuysen

Another suggestion for the humins structure and the mechanism of their formation was proposed by van Zandvoort et al.[103] The structure proposed in this study appears to be more complex compared to previous reports (Fig.2). According to the Weckhuysen group, humins are produced from a combination of formic acid, LA, DHH, and HMF. A model of humins structure was proposed based on extensive analytical investigations using a combination of techniques such as FT-IR and solid state/solution NMR (Scheme 6). Following extensive NMR studies of ^{13}C labelled humins, using a combination of 1D and 2D NMR techniques, the authors determined that glucose-derived humins present mainly Cα–C aliphatic and Cα–Cα linkages, and in a minor amount Cβ–C aliphatic and Cβ–Cβ bonds (Scheme 6).[102,109] The ketone moieties detected can be the result of LA incorporation into the humins structure or from intermediates of sugar dehydration/HMF rehydration.

5.3. Humins formation and composition in biphasic and organic solvent systems

This subject covers a wide range of process conditions, e.g. the addition of water-miscible solvents such as DMSO, the use of "pure" organic solvent systems such as methanol and ethanol, bi-phasic systems such as DCM and water, as well as the use of ionic liquids. These systems have been extensively studied for the production of HMF and to a lesser extent LA. The co-produced humins (which are often observed in smaller amounts than in the pure aqueous systems discussed in the Section 4.3) are less well characterised. It should also be kept in mind that during the dehydration of carbohydrates substantial amounts of water are formed, so none of the reaction conditions described here are remaining water-free.

5.3.1. Mechanism of humins particle growth in water/organic solvent systems

Tsilomelekis et al. reported an investigation of molecular structure, growth rate, and reaction mechanism for humins derived from acid-catalysed dehydration of HMF in water and in water/DMSO mixtures.[22] Using FT-IR analysis, it was observed that the absorbance of the C-H out-of-plane mode relative to the furanic hydrogen stretches decreases after long reaction times. Also, the decrease of the C=O stretch at 1668 cm^{-1} was consistent with previous literature mechanisms involving the

aldol condensation reactions between the enols from DHH and the carbonyl group of HMF that lead to humins.
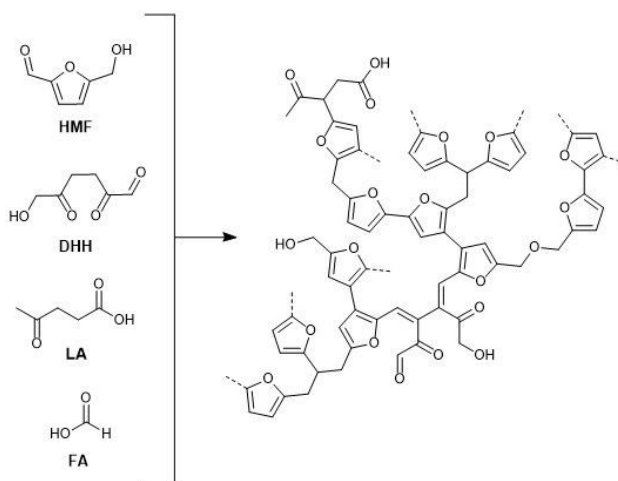
Scheme 6. Humins building blocks and structure as proposed by van Zandvoort et al.[102] and adapted Coumans et al.[223] Reproduced from Coumans et al.[223] with permission from ACS, copyright 2025.

The authors concluded that humins formation involves multiple parallel reaction pathways including substitution at the α or β position of the furan ring via nucleophilic attack, as proposed by van Zandvoort et al.[102] When DMSO was used as co-solvent, nucleophilic attack appeared to be suppressed, leading to smaller humins particles (~100 nm). Using water as solvent resulted in larger particles (between ~100 nm and 5 μm), formed by the aggregation of smaller ones. Humins particles growth in water was studied in situ using dynamic light scattering (DLS).[22] At pH = 0 and 50 °C the initiation of the reaction, associated with the presence of smaller particles (100 – 200 nm), was observed after 10 minutes, while at pH = 1, it was observed after 1 hour (growth rate 2.1-2.9 nm min^{-1}). The key parameters in humins production, as always, were temperature, reaction time, and acid concentration.[103,108] Higher temperatures and acid concentrations led to accelerated growth rate and a greater particle size. Based on these observations, a reaction network for humins formation from HMF in presence of an acid catalyst was proposed. First, soluble oligomeric chains of humins are formed via etherification and aldol condensation reactions as previously discussed.[73,108,125] HMF then reacts with the intermediates (DHH, DHH-like molecules, and/or HMF) and, in aqueous media, the humins particles grow via nucleophilic attack on the furan ring as described above.[103] It is possible to suppress this path by using polar aprotic co-solvents such as DMSO, which cause the particles to remain at reduced dimensions. Finally, small particles combine to produce larger, water insoluble aggregates that precipitate. This reaction network gives a good overview and interpretation of all the results and insights obtained so far on humins particle growth. Fu and co-workers[143] concluded that the degradative condensation of fructose is very much solvent dependent because of different tautomeric preferences in various solvents. Depending on the polar aprotic solvent used,

carbohydrates can exist in pyranose, furanose or acyclic forms. This results in different products originating from dehydration, C–C cleavage and condensation reactions of degraded fructose fragments, explaining some of the possible reaction pathways for the formation of humins during the dehydration of fructose to HMF. Typically, α-fructofuranose in 1,4-dioxane and acyclic, open-chain fructose in THF undergo conversion to formic acid and oligomers, and α-fructopyranose in γ-valerolactone or N-methylpyrrolidone favours formation of LA and oligomers, whereas β-fructopyranose in 4-methyl-2-pentanone favours conversion to acetic acid and corresponding oligomers. These correlations provide a general understanding of the solvent-controlled formation of the oligomers, which represents an important step towards the rational design of effective solvent systems for HMF production.[143]

5.3.2. Humins produced in alcoholic solvents

Humins formed in alcoholic solvents are usually highly viscous, soluble in organic solvents, and less condensed compared to humins originating from aqueous reaction systems. Constant and co-workers recently reported an extensive characterisation of industrial humins derived from pilot plant-scale methanolic cyclodehydration of D-fructose to 5-methoxymethyl-2-furfural (MMF), as part of the Avantium YXY® process to produce FDCA.[48] The authors extended the multi-technique analytical approach previously developed for industrial lignins[224] to these soluble humins. These industrial humins were first purified to remove HMF and MMF and fractionated to allow the isolation of a water-insoluble, high molecular weight fraction, also called Water-Insoluble Purified Industrial Humins (WIPIH), and a water-soluble, low to middle molecular weight fraction, i.e. the Water-Extractable Solubles (WES). These fractions were characterised using a broad range of analytical techniques including elemental analysis, thermogravimetry, size exclusion chromatography, and IR and NMR spectroscopy (solid state-NMR, solution-state NMR with ^{1}H, ^{13}C, [^{1}H, ^{13}C] HSQC, ^{19}F and ^{31}P). Aided by a comprehensive library of NMR spectra of furanic model compounds, the authors assigned the 2D HSQC NMR spectra and identified the main furanic building blocks and inter-unit linkages of the industrial humins (Fig. 4, Scheme 7). The WIPIH and WES fractions were found to be composed of furanic rings interconnected by short aliphatic chains containing a wide range of functionalities including alcohols, ethers, carboxylic acids, esters, aldehydes, and ketones. WIPIH, with an average molecular weight (Mw) of 2250 g/mol, was composed of furanic rings connected with aliphatic linkers via ester or ether bonds. Based on HSQC NMR, there was no evidence of acetal or bis-furylmethane-like units in WIPIH. The most abundant functionality quantified was hydroxyl groups, at around 2.5 mmol per g of humins. Quantification of the total carbonyl moieties using derivatisation with 4-(trifluoromethyl)phenylhydrazine followed by ^{19}F NMR analysis[126] revealed about 1.62 mmol C=O per gram of humins, which represents 4.5 wt% of the WIPIH fraction. It was estimated that carbonyls were mainly present as conjugated enones with roughly only 20% of the carbonyl groups being aliphatic.

In WES, acetals, ethers, and esters appeared to be the main linkers of furanic rings and residual sugar oligomeric derivatives. An average Mw of 470 g/mol and up to 3.9 mmol of hydroxyls per g of humins were measured. Based on these findings and using a top-down approach, the authors revised and refined the previously suggested model[102] and proposed a new model for the molecular structure for industrial fructose-derived humins fractions (Scheme 8). The linkages in the proposed structure result from aldol condensation, etherification, or esterification of the carbonyl, alcohol, and acid groups present in the humins and their precursors. The presence of methanol in the reaction mixture from which these humins originate also led to the insertion of methyl and methoxy groups in the structure. This methanol incorporation likely inhibited further dehydration/condensation reactions and resulted in a lower degree of cross-linking compared to aqueous reaction mixture-derived (synthetic) humins. Shi *et al.*[122] also observed that very limited amounts of solid humins were formed using ethanol as solvent. Through acetalisation, ethanol was suppressing condensation reactions of the main humins precursors (α-oxo aldehydes and α,β-unsaturated aldehydes) and thus limiting humins formation. In addition to the characterisation work, Constant *et al.* also studied the relationship between industrial and synthetic humins.[48] By conducting an aqueous acid thermal treatment at 180 °C on the industrial humins, it was shown that the industrial sample was structurally related to more recalcitrant insoluble humins and can be possibly considered a precursor of these materials. Filiciotto *et al.*[146] reported a study of the interpretation of humins chemical structure based on bottom-up approaches. Industrial humins were subjected to catalytic decomposition (thermal and hydrogen-assisted reactions) in continuous flow and the resulting products were subsequently analysed. This approach was based on decomposition of the humins into detectable products which subsequently could be associated with potential building blocks, called reconstruction.[146] A plethora of products were isolated in this process, underlining the high complexity of the humins structures. The identified products included furanics, levulinates, sugar derivatives, aromatics, small organic acids, and several other oxygenated molecules. Contrary to previously proposed humins structures, this reconstructed structure points to a more heterogeneous composition and is similar to that of a hydrothermal carbon.[150,167] However, the approach needs to be further verified. Another methodology reported by Sangregorio *et al.* involved a study of the curing kinetics of these industrial humins in order to gain insights into their general condensation process.[142] Thermally treated humins showed an auto cross-linking behaviour and the process was faster when an acidic initiator was used.
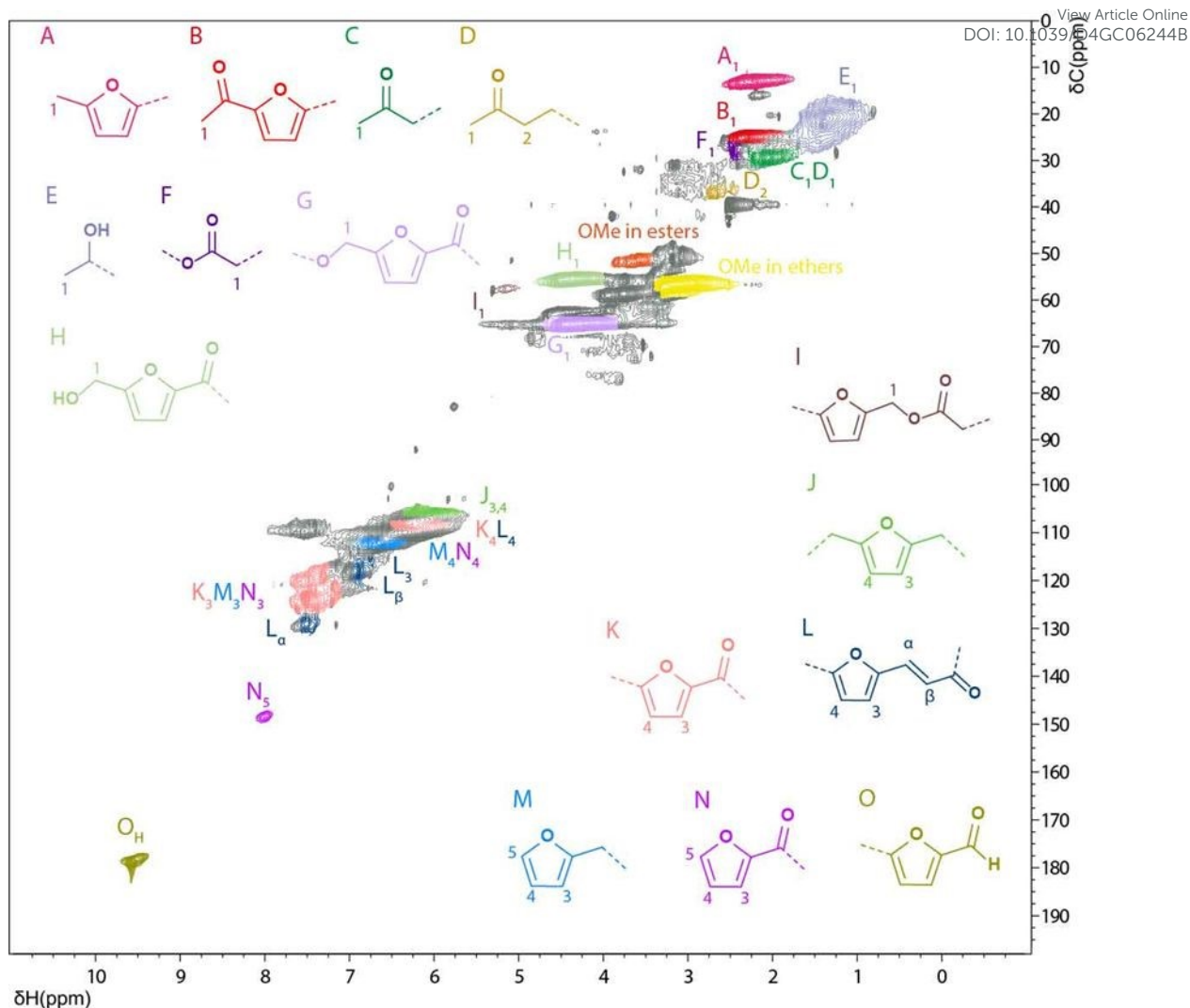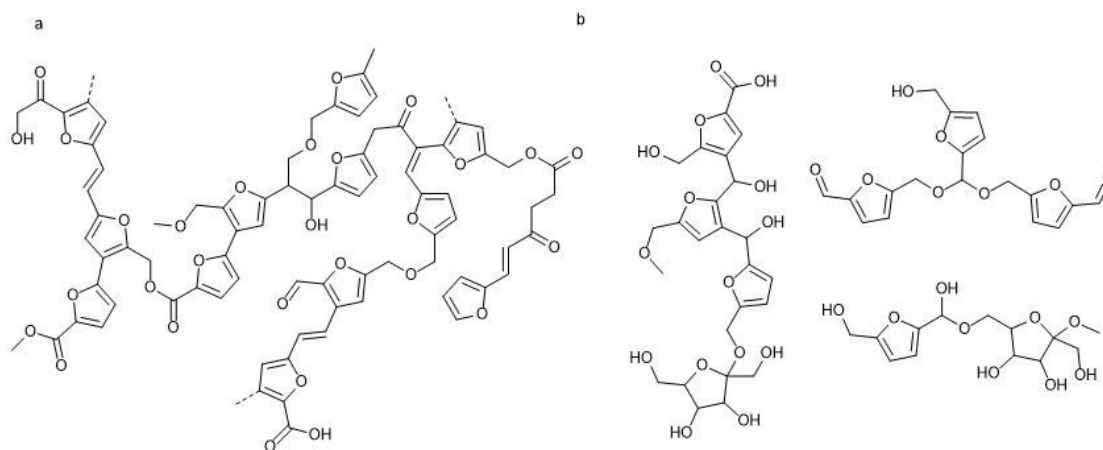
Figure 4. Solution state [^{1}H; ^{13}C] HSQC NMR spectra of water-insoluble purified industrial humins (WIPIH) in d$_6$-DMSO with the main synthons/structures identified.[48]

Scheme 7. Revised model for the molecular structure of industrial fructose-derived humin fractions; (a) representation of the WIPIH high molecular weight fraction, (b) representation of the water-extractable solubles (WES) low to middle molecular weight fraction.[48]
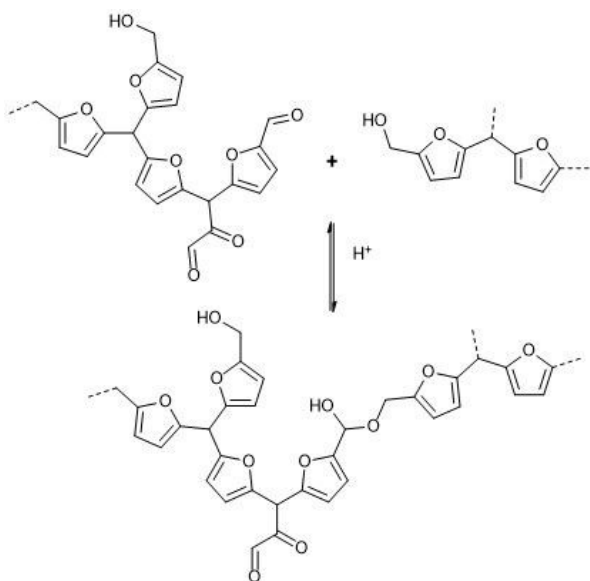
Scheme 8. Acid-catalysed hemiacetal formation between humins chains.[142]

This phenomenon allows faster cross-linking at lower temperatures, which is important for many of the applications discussed in Section 6. It was postulated that the cross-linking occurs via an acid-catalysed hemiacetal formation pathway (Scheme 8).

Cerdan *et al.* studied the thermal polymerisation mechanisms of similar industrial humins from a rheological perspective.[225] They also observed that thermal cross-linking of native industrial humins led to an increase in molecular weight and subsequently to the formation of a gel, the structure of which was composed of physical (thermally reversible) and chemical (thermally irreversible) cross-links. Temperature played an essential role in the cross-link density and the gel properties. High temperatures hampered gel formation and markedly decreased viscosity, whereas upon cooling a stronger gel was formed by restoring the physicochemical bonds via the formation of chemical cross-links. In addition, a transition from a supramolecular network to a covalently cross-linked network was observed, and properties such as elasticity and reprocessability of humins gels were influenced by the degree of polymerisation.[225] The low level of cross-linking together with the high content and diversity of functional groups of humins formed in alcoholic solvents allows for a broader range of valorisation opportunities compared to more condensed humins (Section 6).[48]

5.3.3. Humins formation in ionic liquids

The mechanism of humins formation from glucose/fructose conversion into HMF was studied in the ionic liquid system 1-butyl-3-methylimidazolium chloride, ([BMIM]Cl) with CrCl$_3$ as catalyst.[140] Furanic model compounds representing the identified humins intermediates were investigated to understand the humins growth mechanism. The authors identified three types of reactions that result from the instability of furan compounds bearing a hydroxymethyl and an electron-donating group and thus promote humins growth: (1) bimolecular ether formation, (2) intermolecular addition, and (3) furan ring cleavage with water. Hydroxymethylated furans could be stabilised in [BMIM]Cl when the OH group was protected as a methyl ether, and the stability was further enhanced by electron-withdrawing groups such as an aldehyde group on the ring.[140] Analysis of humins formed in ionic liquids showed that the structure and morphology do not resemble those reported in literature, and that the material displayed a number of unique aspects. The hydrogen bonding proprieties of the ionic liquid exert a strong influence on the chemical functionality of the humins generated in their presence, and this may give them advantages as functional materials.[226]

5.4. Humins formation and composition produced under hydrothermal carbonisation conditions

Highly cross-linked humin-like substances are produced by hydrothermal treatment of pure carbohydrates as well as lignocellulosic biomass, leading to so-called hydrothermal carbons (HTCs).[133,134,154] The hydrothermal carbonisation approach is widely used to produce carbonaceous compounds.[167,227] In contrast to the acid-catalysed dehydration humins, HTCs are in general formed without the addition of mineral acids and are the targeted product of hydrothermal biomass treatment. The hydrothermal carbonisation of carbohydrates is carried out by the combined application of temperature and pressure usually at 130-220 °C.[150] HTCs can be considered as fully reticulated, solid humins produced as structured micro- and nano-particles that may have applications in several fields, including catalysis and catalyst supports, soil enrichment, energy storage, water purification, and CO$_2$ sequestration.[105] HTC materials have been extensively studied, and their characterisation can be used as a reference model for acid-catalysed dehydration-derived humins.

FT-IR, NMR, and/or Raman analysis of HTC derived from fructose, glucose, and HMF showed the presence of aromatic structures.[147,151,153] Observations of ^{13}C labelled HTC using advanced solid-state ^{13}C NMR showed that HTC contains furan-based substances. The various subunits are linked together through aliphatic chains in the α or β positions of the furan ring with hydroxyl and carbonyl moieties also embedded in the structure (Scheme 9).[150,154] Similarly to humins, the HTC structure differs depending on the feedstock. In their series of articles, Titirici and Baccile suggested different structures for pentose- and hexose-derived HTCs.[147,154,156] HTCs derived from hexoses (including glucose and fructose) were similar to each other, but differ slightly from pentose-derived HTC.[147] Indeed, HTC from xylose had lower H/C and O/C ratios compared with HTCs from other sugars.[147] HTCs from C5- and C6-sugars result in similar compositions to those obtained from furfural and HMF. The difference between HTCs derived from pentoses and hexoses can be explained by the different H/C and O/C ratios of the primary building blocks, e.g. furfural (C$_5$H$_4$O$_2$) and HMF (C$_6$H$_6$O$_3$). Thus, the ^{13}C NMR spectra of xylose-HTC contained fewer aliphatic groups, along with stronger signals associated with C=C conjugated systems compared to glucose-HTC. C6

Journal Name

ARTICLE

sugar-HTCs and HMF-HTC were quite similar, while C5 sugar HTCs were closer to carbonised furfural.[103] The structure of HTC, like in acid-catalysed dehydration of humins, appears to be strongly dependent not only on the feedstock used but also on the preparation temperature.[156] Sugar-derived HTC prepared at 180 °C consisted of a furanic network with aliphatic linkers, as reported above.[154] However, in sugar-derived HTC calcinated at 350 °C, a higher number of conjugated aromatic rings was found, generated by aromatisation and furan ring fusion to give polycyclic systems. When HTC were prepared above 400 °C, they resembled graphene-like sheets.[156] Thermolysis of HMF at 27.5 MPa and 290 to 400 °C led to furfural, a residual humic "tar," and 1,2,4- benzenetriol in yields of up to 46%.[83]

Regarding the HTC mechanism of formation, a series of reactions including dehydration, polymerisation, and aromatisation were proposed by Baccile *et al.*[127] and Eady *et al.*[228] and are shown in Scheme 10. Part of the HTC originates from the dehydration of C6-sugars into HMF and C5-sugars into furfural, and some of the furanics subsequently undergo ring opening reactions to give diketones.[127] Thus, aldol-like condensations and aromatisation via Diels-Alder reactions along with polycondensations lead to the HTC structure. Shi *et al.*[121,122] suggested a pathway for HTC formation involving aldol condensation, subsequent acetal cyclisation, and dehydration using α-oxo aldehydes (such as 3-deoxyglucosone) and α-oxo carboxylic acids as precursors. Another parallel route proposed by the authors was a Cannizzaro-type reaction to form α-hydroxy acids.[121,229] The initialisation of the polymerisation of HTC is followed by the nucleation and growth of spherical particles by the incorporation of HMF/furfural-derived molecules.[150] The HTC could have a uniform particle size,[148] or a wide distribution of particles sizes,[147] or have no defined shape.[149] The HTC polyaromatic spherical structures are composed of a hydrophilic shell and a dense hydrophobic core.
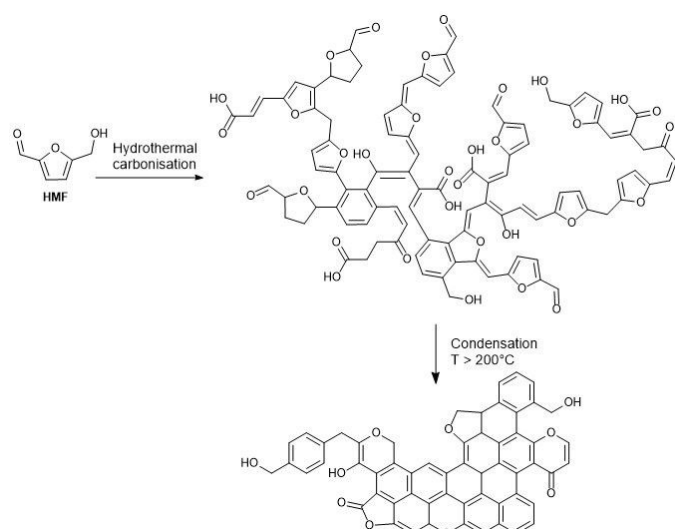
Scheme 9. Conversion pathways of cellulose derived HMF into acid-catalysed dehydration (ACD) humins[102,103] and hydrothermal carbons (HTC).[150]
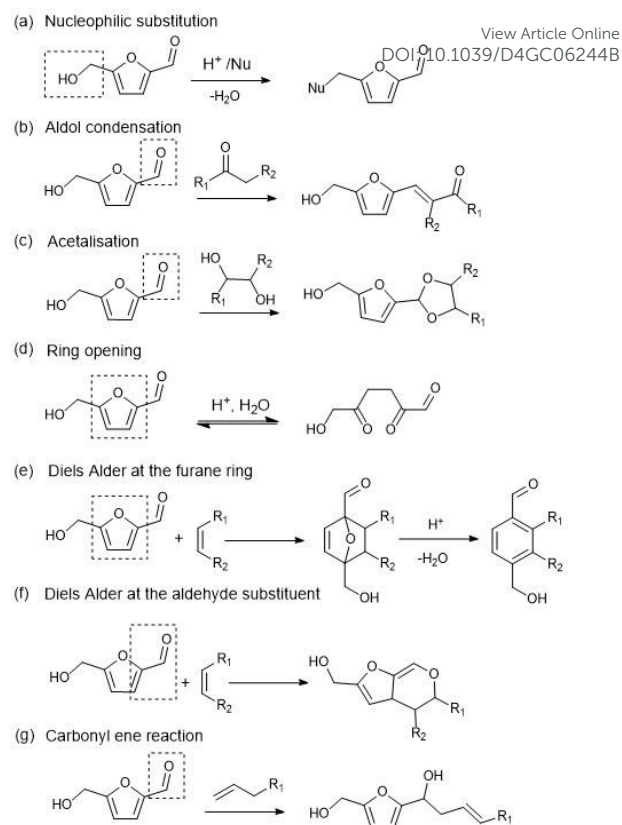
Scheme 10. Possible chemical reactions of HMF, including diketone (DHH) formation (reaction d), during the hydrothermal carbonisation process. Redrawn and adapted from Baccile *et al.*[127] with carbonyl ene reaction (g) from Yue et al.[230] and Eady et al.[228] with permission from Wiley, copyright 2025.

Sevilla *et al.*[133,134] showed that the diameter of spherical HTC particles can be modulated in the range 0.4 – 6 µm by controlling the reaction parameters, such as temperature, reaction time, feedstock, and concentration. A temperature increase was associated with an increase in the C/O and C/H ratios due to carbonisation and aromatisation of the structure. This was supported by a decrease in oxygen moieties as determined by FT-IR. Slight differences between the bulk and surface were observed by TEM. Similar C/O ratios, with several oxygen groups present at the surface and in the bulk material, were analysed by XPS.[133,134] Different morphologies were observed on the surface of HTC particles depending on the starting monosaccharide (textured when produced from glucose, smooth when produced from fructose).[151] HTC can also be formed around a metallic nanoparticle centre, and the surface can be decorated with smaller metal particles such as Ag or Pd.[148] Specific new functionalities can be introduced onto the surface of HTCs by taking advantage of the exposed reactive moieties.[231,232]

This section has shown that in the last two decades a lot of fundamental information on humins formation and composition has emerged, although the picture is far from complete. More work is needed on the molecular mass determination of (soluble) humins, the influence of the feedstock source on humins properties, and better

ARTICLE

understanding of the reactions that occur during the processing of reactive humins. To make humins suitable for higher-value applications it is also important to understand how the properties of humins can be steered towards the desired functionalities. The current status of these value-added applications will be discussed in the next section.

6.   Value-added applications for humins

The development of suitable applications for acid-catalysed, dehydration-derived humins was underdeveloped for a long period of time, if even considered at all. However, in the last decade several studies have been conducted focusing on the potential applications of these industrial side-products, many with promising results (Fig. 5). There is already a wide range of uses under development, from solubilisation, gasification, and the production of syngas to use in self-healing materials for robotics. Research in application development is growing fast, and the investigations around this emerging topic are both encouraging as well as very much needed, because as described earlier, humins appear to be unavoidable as side-products in the ubiquitous acid-catalysed processing of carbohydrates. Improvement of the business value proposition for industrial humins is therefore a necessity for the development of a truly circular, biobased economy. The use of furan-based resins for various applications is long established, and Gandini and co-workers have published an extensive review of the current state of the art on this subject.[233,234] Resins based on furfural and furfuryl alcohol currently represent the most important products within this context, but polymers based on HMF and 5-methylfurfural have also been discussed.[233,234]

6.1. Solubilisation and modification of humins

In order to make humins processing and transportation easier, solid humins should ideally be solubilised or, if liquid, be available in a less viscous phase.[235,236] However, the solubility of these recalcitrant side-products is generally quite poor. For instance, solid humins formed via acid-catalysed dehydration in water showed only a 3-5% weight loss after 24 hours of Soxhlet extraction with acetone and ethanol.[124] Thus, there is a growing interest in making humins more soluble and easier to process.[235]

Fig. 5. An overview of potential industrial applications of humins currently under investigation.

Van Zandvoort performed the reactive solubilisation of humins using an alkaline pretreatment similar to that used for lignin.[109] Glucose-derived humins were solubilised in 0.5 M NaOH at 200 °C for 3.5 h, while xylose- and fructose-derived humins required a higher temperature of 240 °C. It was observed that longer treatment times and higher temperatures led to a reduction of the average Mw. 0.5 M NaOH was selected as the best medium, since a stronger alkaline environment leads to a greater decrease in the Mw. These investigations were performed using a combination of techniques (solid-state NMR, elemental analysis, FT-IR, GC-MS). This work suggests that alkaline treatment leads to the cleavage of C-O-C bonds, and thereby to the reduction of the Mw. An increase in aromatisation of the material (presumably via Diels-Alder and/or dehydration reactions) was also detected, which leads to polycyclic systems bearing carboxylic groups.[109] Indeed, FT-IR signals associated with carboxyl functions increased at the expense of ketone groups, and this structural change (along with the reduction of the Mw) could explain the increased solubility of humins after such treatment. The humins obtained by this method were soluble at pH > 7 and could find applications in the production of syngas or hydrogen via aqueous phase reforming or catalytic hydrotreatment.[237–239]

A simple and industrially relevant way to solubilise humins by acelation was reported Mija et al.[235] The reaction of humins with a series of maleic, succinic, valeric, or stearic acid anhydrides, organic acids (acetic acid, sebacic acid), or acyl halide (stearoyl chloride) gave good yields of low viscosity acylated humins. The modified humins were less hydrophilic so they become more suitable as potential biofuels. This process can also facilitate humins transportation as the acylated humins have manageable viscosity values in the range 5 to 40 Pa·s at 60 °C. A selective chemical modification of industrial humins was recently reported to alter their physical properties.[240] Thus, esterification of humins into humins-benzoate, -acetate, and -valerate derivates was conducted to suppress hydrogen bonding and give the product in a powdered form. In contrast, low viscosity humins liquids (200 Pa·s) were obtained using adipoyl and sebacoyl chlorides.[240] The solubilisation of humins using solvents of different polarities was studied by Cheng et al.[138] The authors confirmed that humins were not simply a high molecular weight polymeric product, but more of a heterogeneous mixture of large, insoluble molecules along with smaller, soluble species. These molecules of different molecular weights interact with each other by weak forces and dipolar interactions. The study showed that solvents with higher donor numbers (higher Lewis basicity) were better solvents for humins, and the solubilised humins could make transportation more convenient.[138]

6.2. Gasification of humins

The potential for the valorisation of humins by steam reforming to give H_2 was investigated the group of Seshan.[135,241,242] Both thermal and catalytic steam gasification were studied. The alkali

metal-based catalyst Na_2CO_3 showed the highest activity and product analysis indicated that the selectivity to CO and CO_2 was 75 % and 25 %, respectively.[242] After the thermal treatment, the remaining humins were modified both in morphology and structure. They consisted of de-oxygenated, highly aromatised char residues with around 45 wt% of sample losses through the generation of volatile compounds. Valorisation of humins via dry reforming was also studied. Non-catalytic dry reforming of humins is challenging under mild gasification conditions (below 1000 °C).[241] Again, Na_2CO_3 enhanced the reforming rate, making the process more viable.[241] Acetic acid and phenols were found to be the major components of the condensable side-products in the low temperature stage of humins gasification.[135]

6.3. Pyrolysis / liquefaction of humins

The pyrolysis of representative solid humins samples derived from fructose and glucose were first assessed by the group of Heeres.[93,132,236,243–245] Pyro-GC–MS (300–600 °C, 10 s, helium mobile phase) and micro-pyrolysis (500 °C, 12 sec, N_2 atmosphere) were used. Using pyro-GC–MS, furanics, organic acids, and other components were produced in small amounts (<1 wt%). Micro-pyrolysis yielded 30 wt% gaseous and liquid products, the remainder being a solid char. Synthetic humins, crude industrial humins, and purified industrial humins showed significant differences in thermal degradation patterns. Thermal decomposition of industrial methanol-based humins was observed between 50 and 650 °C (66 wt% weight loss), whereas the major weight loss for the more condensed synthetic solid humins (47 wt%) was between 200 and 800 °C. For quantitative analysis, a gram scale pyrolysis unit was used, giving product oils (9–11 wt% with respect to humins load) with approximately 1.5 and 10 wt% aromatics arising from synthetic and crude industrial humins, respectively. GPC analysis on the product oils clearly showed the breakdown of the humins structure into lower molecular weight species. The higher heating value (HHV) of the liquid products (up to 41 MJ kg^{-1}) was considerably higher than the crude industrial humins feed (21–24 MJ kg^{-1}).[246] Recent work of the Heeres group reports on the catalytic pyrolysis of technical humins derived from pyrolytic sugar oil.[245] Mixtures of benzene, toluene, xylene naphthalene, and ethylbenzene in 5.1 wt% yield based on humins loading were obtained. Batch liquefaction experiments at 350 °C for 4 h with isopropanol as both the solvent and hydrogen donor resulted in 80 wt% conversion of the humins feed into a product oil with considerable amounts of phenolics and aromatics (24.7 % based on GC analysis).[245]

Vlachos and co-workers[247] reported a one-step catalytic hydrotreatment of humins in methanol into humins oil containing fully and partially deoxygenated compounds using commercial noble-metal catalysts. Aromatic hydrocarbons, phenols, and esters were the main products. The highest oil yield and a conversion of 75% were obtained at 400 °C for 3 h at 30 bar H_2 using a catalyst-to-humins mass ratio of 1:10. ^{13}C-isotopic labelling studies confirmed that methanol participates in alkylation and esterification reactions, incorporating into aromatic, phenolic, and ester products.[247]

Similarly, the catalytic conversion of humins into cyclic hydrocarbons was reported with a 95% conversion rate and up to 88% yield using a bifunctional catalyst.[248] The C–C bond network was efficiently depolymerised at reaction temperatures of 340–380 °C under the cooperative catalysis of nano-Ru particles and a porous, strong Lewis acid.[248] The catalytic hydrotreatment of humins using supported Pd @ zeolite (Beta, Y, and USY) catalysts with different amounts of Pd was investigated under hydrogen pressure. The major compounds in the humins oil as shown by GC-MS were alcohols, organic acids, ethers, and alkyl-phenolics.[249] Furanic compounds were not identified in the reaction products. A possible explanation may be related to their high reactivity under the reaction conditions.

Finally, preliminary studies of spray combustion of humins / ML mixtures as an alternative to heavy fuel oil (HFO) have also been conducted.[250] It was reported that parameters such as stability, heating value, flashpoint, viscosity, and density of these mixtures fall within the HFO limits. In the spray combustion tests, the mixture had ignition and combustion behaviours similar to HFO. However, the combustion residual ash and carbon were high, representing risks in terms of engine damage, while determination of the calculated carbon aromaticity index (CCAI), acid number, and water content was not possible because of the oxygen content of the humins/ML fuel.[251] Another potentially interesting valorisation methodology involving catalytic hydrotreatment of humins was reported using ruthenium catalysts at 400 °C in presence of FA and isopropanol or H_2. Up to 69% conversion was obtained in the best case, resulting in an oil consisting mainly of monomers (principally alkyl phenolics) and small oligomers.[236]

6.4. Oxidised low molecular mass compounds from humins

The catalytic oxidation of humins with O_2 into short-chain carboxylic acids was reported using homogeneous polyoxometalate as catalyst under mild conditions (90-120 °C).[252] Unfortunately, low yields of formic and acetic acid resulted. For example, only 8.3 wt% and 4.0 wt% were respectively obtained, the main product being CO_2. Comparable yields were reported later by Wassenberg.[128] The same authors further investigated the oxidative conversion of humins using model substances like furan derivatives of varying complexity in combination with polyoxometalates as oxidation catalysts in aqueous media.[253,254] Various transition metals such as V, Mn, Co, Ni, and Nb were used as substitutes for molybdenum atoms in Keggin-type phosphomolybdates. The $H_4[PVMo_{11}O_{40}]$ catalyst showed the highest activity and lowest CO_2 formation.[253] A two-step degradation of humins was studied by Kang et al.[255] involving alkaline catalytic hydrothermal treatment and wet oxidation. Acetic acid yields of 37.2% on a mass basis in water were achieved.

6.5. Activated carbon from humins

A new class of highly porous organic sorbents called microporous humins can be produced from humins, which in

some cases have high levels of CO_2 sorption, and thus could potentially be useful for the separation of carbon dioxide from gas mixtures.[256] Their synthesis involves the polymerisation of HMF in concentrated sulfuric acid and treatment with diethyl ether and heat, by which the porosity could be tuned. A high uptake of CO_2 (up to 5.27 mmol/g at 0 °C and 1 bar) and high CO_2-over-N_2 and CO_2-over-CH_4 selectivities were observed. These microporous humins were aromatic in nature and structurally amorphous, which was shown in a multipronged approach using ^{13}C NMR, FT-IR, elemental analysis, and WAXS.[256]

Microporous humins-based materials were also prepared by Björnerbäck and Hedin.[257] In this case, humins of controlled porosity were produced by acid-catalysed dehydration of sugars with concentrated sulfuric acid. The humins were then washed with ether and carbonised at 400 °C. Despite the interesting results, these processes do not aim directly at the valorisation of industrial humins, because they involve the targeted synthesis of humins following a specific protocol. It would be interesting to evaluate whether the findings of these studies can be applied to industrial humins.[257]

The preparation of humins-derived activated carbon at 800 °C was reported by Kang et al.[258] for sorbent material applications. A pseudo-second order kinetic model was developed to simulate the adsorption capacity, with a maximum of 1195 mg g^{-1} of methylene blue and 218 mg g^{-1} of phenol.[258] The principal reason for such high adsorption capacities was associated to the pore size distribution (1.7 – 300 nm). It was also suggested that acid groups, with a density of 3.3 meq g^{-1} on the macroporous surface, also contributed.[259–263] Additionally, preparation of activated carbons from humins using phosphoric acid activation has been reported, achieving a BET surface area of 2375 m^2 g^{-1} under optimal conditions (400 °C).[258]

Other preparations of activated carbons of previously carbonised humins were investigated using both physical (CO_2) and chemical activation (KOH), including tests as supercapacitor electrode materials.[264] Unfortunately, good characterisation of the texture of the activated carbon produced was lacking, while the BET surface area was poor compared to commercially available carbons (862 m^2·g^{-1} in the best case).[265] However, the electrochemical characterisation of these humins-derived activated carbons using a 3-electrode cell showed that they potentially have promise. Al Ghatta et al.[226] found that humins produced in various ionic liquid environments can be used for metal extraction, having comparable efficiencies to commercial activated carbons. For example, this study revealed that humins were superior for the extraction of antimony from wastewater, showing promise as an adsorbent additive for water purification. Vinod and Dutta used humins-derived activated carbon (HAC) for the phosphotungstic acid-catalysed esterification of LA into alkyl levulinates[266] as well as the synthesis of gamma-butyrolactone by catalytic hydrogenation over palladium supported on HAC.[267]

6.6. Humins as catalyst (support)

Humins-based iron oxide nanocomposites have been reported as catalytic materials.[268] Humins were also used as templates

for the synthesis of alumina foam catalyst supports.[269] The catalyst was prepared using cheap and solvent-free methodologies, using both crude industrial humins and humins foams. These catalysts were tested in the microwave-assisted synthesis of vanillin from isoeugenol in an oxidative environment and showed good recyclability in some cases. After only 5 minutes, vanillin yields between 42-57% were achieved. When multifunctional sulfonated humins (MSH) were used as the catalyst in 90 wt% aqueous sulfolane solution, cellulose was converted into LA in 65.9% yield. The MSH exhibited outstanding performance both in catalytic activity and recyclability due to its synergistic effect with sulfolane and water. A levulinic acid yield of 45.6 mol % was likewise obtained starting from bamboo instead of pure cellulose.[270] Yang and co-workers[271] described the use of glucose-derived humins as the starting material for a novel class of effective carbonaceous solid acid catalysts produced via low-temperature pyrolysis followed by sulfonation. A range of reaction conditions were investigated, and the structure-function relationships of the resulting catalysts were also discussed based on the analysis of the structure and composition. Compared to a catalyst derived simply by the carbonisation of glucose itself,, the humins-derived catalyst had a substantially greater surface area and higher SO_3H density, which enabled it to show higher catalytic activity and efficiency, not only in esterification of levulinic acid and n-butanol (yield = 95 %, 373 K), but also in hydroxyalkylation/alkylation of 2-methylfuran and furfural (yield = 64.2%, 323 K). Additionally, the catalyst could be reused over at least four cycles without obvious deactivation.[271] Galaverna and co-workers[272] reported a new humins-like resin, prepared from 2,5-bis(hydroxymethyl)furan (BHMF, Fig. 2) and maleic anhydride, which was used as a solid support for palladium immobilisation. Proof of concept was demonstrated using Heck and Suzuki cross-coupling reactions. The activity (yields up to 99 %) and reusability (at least 7 times) of the catalyst were evaluated. A different approach was pursued by Queen and co-workers, who presented a scalable, solid-state method for metal-organic framework (MOF)/polymer composite production.[273] The simple method consists of mixing a MOF powder, namely Fe-BTC (BTC = 1,3,5-benzenetricarboxylate), with HMF and heating the resulting solid, which promotes both solid-state diffusion of HMF into the MOF and the formation of a humins polymer with a high density of accessible hydroxyl functionalities within the MOF pores. The resulting composite, Fe-BTC/humins, was found to selectively extract Ag^+ ions from laundry wastewater. Subsequent reduction of the Ag^+ species yielded a novel catalyst, Fe-BTC/humins/Ag, which was able to catalyse the reduction of cinnamaldehyde into cinnamyl alcohol in a highly selective manner. Moreover, the catalyst exhibited recyclability up to five cycles, which is an improvement over the Fe-BTC/Ag catalyst without humins.[273] Solid humins derived from starch-rich waste were valorised as raw materials for producing biochar-supported Lewis acid catalysts. These humins were collected and impregnated with $AlCl_3$ followed by carbonisation. Detailed characterisation revealed several aluminium oxide species on the biochar surface, plausibly in the amorphous state. These

ARTICLE

humins-derived biochars exhibited good catalytic activity toward glucose-to-fructose isomerisation, a common biorefinery reaction in the dehydration of carbohydrates catalysed by Lewis acids.[274]

A porous lignin-humins composite was produced as a side-product of the acid-intensive CMF process on raw biomass (spruce sawdust).[275] The powdery solid that was filtered from the reactor already had a moderate level of porosity which dramatically increased on pyrolysis above 400 °C. The most interesting property of this humic material was its mesoporous pore structure with a width distribution of 30 ± 20 nm. Most pyrolytic carbons, on the other hand, are microporous (pore width < 2 nm). Mesoporosity is a highly desirable property in catalysts as it provides good accessibility to active sites, as opposed to microporosity, which tends to impose diffusional control because of the restrictive pore volumes. Samples of the product were sulfonated to test their potential as heterogeneous acid catalysts in the esterification of levulinic acid with ethanol. The unpyrolysed sulfonated catalysts gave the highest ester yields (up to 92%). Origin Materials is currently commercialising materials of this kind as a co-product of CMF production.[61]

6.7. Humins as components for asphalt

To decrease the environmental impact of bitumen, more sustainable binders are being developed. It was shown that industrial humins can be used as a macromolecular binder for bitumen.[276] Humins were mixed at 50 wt% with bitumen. When the non-water soluble fractions of humins (Humins Non Soluble - HNS) were employed, no variation in the chemical structure of the bitumen was observed in FT-IR spectra after the mixing. DSC investigations showed that the crystallisation of the aromatic fractions in bitumen shifted to higher temperatures in humins-modified bitumen. The thermogravimetric data highlighted that the presence of humins or HNS in bitumen can lead to higher mass loss below 200 °C compared to pure bitumen. Rheological investigations highlighted some key advantages of adding humins or HNS into bitumen. At high temperatures, the storage modulus of the modified bitumen is increased and shows lower susceptibility to variations in frequency in the viscosity measurements. At low temperatures, the phase angle of HNS-modified bitumen is lower than that of bitumen, suggesting less temperature dependent viscosity changes as a consequence of a cross-linked network formation.[276] Also, a patent application has been filed on an asphalt compositions that include humins, claiming improved wet- and dry-strength properties.[277]

6.8. Humins-based adhesives for fibre-based materials

Another humins application that has been studied is as thermoset resins and in material composite preparations. For instance, thermosetting resins were obtained by adding large quantities of humins (55-75%) to a polyfurfuryl alcohol (PFA) network.[111,112] The preparation was carried out by acid-induced polymerisation, and the chemical interaction between the PFA and the humins was followed by FT-IR analysis. This furan-based resin mixture was impregnated on cellulose fibres for the production of fibre composites after curing. It is worth noting that the tensile strength of these humins-PFA composites was twofold higher than other composites made from PFA or PFA-lignin. Humins-PFA composites were less brittle compared to their common FA-based analogues due to enhanced interactions between the resin and the fibre.
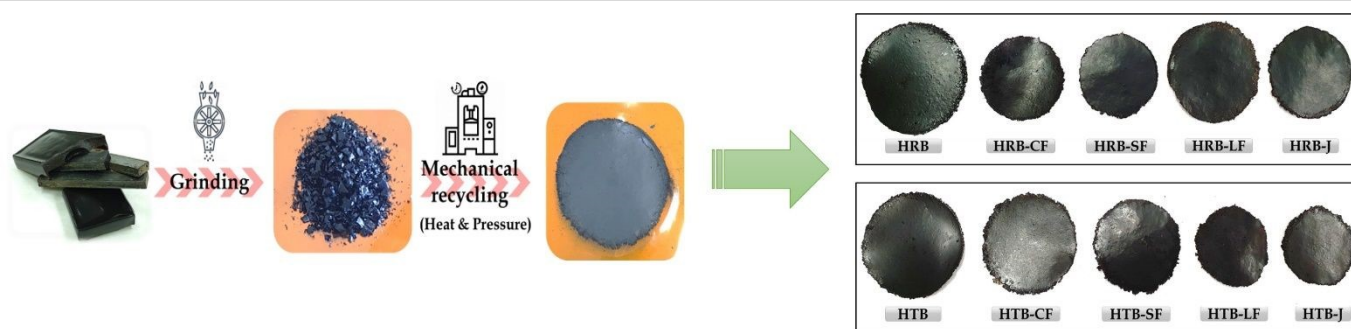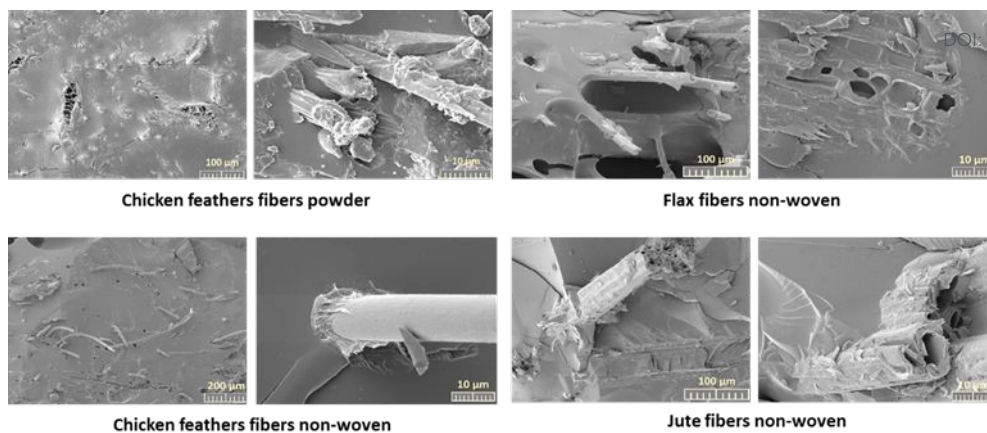

Fig. 6. Reprocessable humins-based thermosets and their composites with chicken feathers or jute, hemp, and flax non-woven fibres.[278] Redrawn and adapted from Dinu et al[278] with permission from Elsevier, copyright 2025.

Fig. 7. SEM analysis showing the strong compatibility between the humins-based thermosets and chicken feathers, jute, and flax non-woven fibres.[278,279]

These materials not only showed interesting properties, but also cost reductions, since lower quantities of FA were required. Kang et al.[280] reported the use of humins as potential low-value phenol replacements in phenol-formaldehyde type adhesives for wood adhesion applications. Humins were first treated hydrothermally in order to produce an alkaline soluble additive which was subjected to reaction with formaldehyde and phenol. The humins-(50 wt%)-phenol-formaldehyde adhesives thus obtained showed good bonding strength and viscosity properties, and met the GB/T 14732-2006 Chinese National Standard safety requirements for commercialisation. Sangregorio et al.[115] reported a study on the reactivity of industrial humins, proving their potential in the preparation of thermoset-like resins and confirming previous results[95,106] that showed that, upon sufficient thermal treatment, humins mixtures were able to react in a non-reversible way, polymerising into a furanic based network. Glass transition (Tg) values above 65 °C were measured after thermal treatments at 120-140 °C. Such Tg values are close to those found for humins foams produced at a higher temperature (250 °C), proving that the completeness of the cross-linking could be associated with a glass transition of 70-75 °C. In the wake of these results, Sangregorio et al. reported the preparation of composite humins-flax fibres.[114,116] These composites proved to have a good elastic modulus of ~1.5 GPa, while SEM showed good adhesion between the humins matrix and the flax fibres (Fig. 6). The only drawback reported was that, despite an interesting reduction in hydrophilicity of the composite material compared to that of pure flax, some furanic compounds could be leached into water (mainly 5-hydroxymethyl-2-furancarboxylic acid (HMFCA)). This might be the result of incomplete curing of the industrial humins and requires further investigation.

Reprocessable humins-based thermoset resins were synthesised for the first time by Dinu et al. by copolymerising humins with a biobased epoxy monomer, either resorcinol diglycidyl ether or trimethylolpropane triglycidyl ether.[278] These bioresins have excellent thermal stability, tensile strengths up to 10 MPa, and Young's moduli up to 1.8 GPa and could be reinforced with the addition of chicken feathers or plant-derived, non-woven (Fig. 7).[278] These composites showed Tg values ranging from 37 to 81 °C, and SEM analysis confirmed very good adhesion and good compatibility between the matrices and the fibres (Fig. 7). Both the resins and composites were able to be mechanically reprocessed without impacting their properties, even after 10 cycles.

Recently, a dedicated humins batch reaction production system was described for adhesive applications.[281] The scaled-up production of HMF-based adhesive precursors used industrially available fructose syrup with sodium dithionite as stabiliser. With this system, no concentration steps are needed in the generation of adhesive precursors for wood composite board production. The synthesised adhesives were tested for particle board applications at the appropriate concentrations.

Vidal et al.[282] reported the production of sustainable composites for construction material applications based on hemp and flax fibres reinforced with a matrix combining humins and epoxidized linseed oil. The thermal conductivities of the

composites were measured to be around 0.1 W/mK, which is in line with other natural materials used in buildings.[62] The composites were tested both for their flame retardancy and the generation of burning drops. The results showed that none of the materials generated burning drops when exposed to fire and they also had a lower tendency to spread fire compared with natural fibres. It also has been reported that melt-spinning of humins into fibres is possible.[283]

6.9. Humins for making wood more durable

Current approaches to increasing the durability of wood, such as treatment with bitumen or CCA (copper-chromium-arsenic), result in an environmental burden, thus more benign and preferably biobased solutions are desired. Recent work has focused on an alternative way to modify wood by impregnation with industrial humins and subsequent curing.[144] Their high affinity with lignocellulosic biomass allowed humins to be polymerised in situ within the wood matrix (Fig. 8). The resulting modified wood showed enhanced dimensional stability after immersion in water without compromising the mechanical properties. From a fire safety point of view, impregnation did not significantly impact the flammability of treated pinewood. Moreover, advantages of humins compared with polyfurfuryl alcohol (PFA) as a wood impregnation agent have been identified both in terms of thermal hazards and fire-induced toxicity hazards. A photodegradation stability study of pine micro veneers modified with humins and 3wt% of citric acid, used as reaction catalyst, showed 41 % lower strength losses in weathered humins-treated wood compared to untreated wood.[284] Modification of wood with humins thus shows promise for improving the properties of lumber in a green and sustainable way.[58,144,235,285]
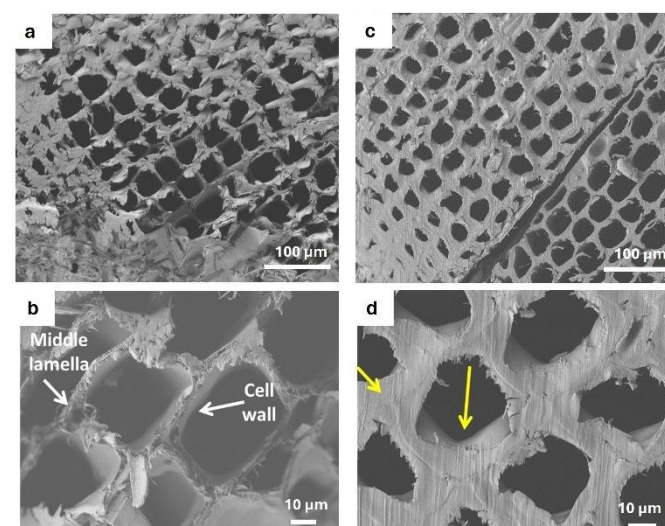

Fig. 8. Scanning electron micrograph (SEM) images taken from the cross-section of control wood (a and b) and humins-modified wood (c and d). Middle lamellae and cell walls are indicated by the arrows.[144]
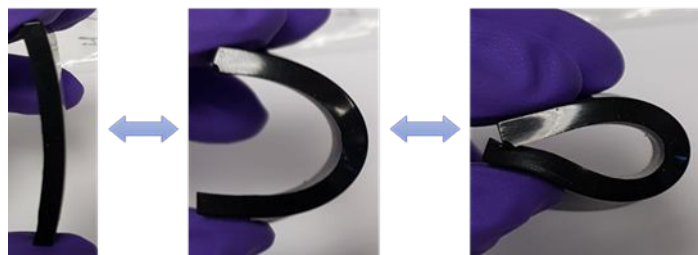
Fig. 9. Different humins-based thermoset behaviour as a function of formulation, from more rigid to more elastic.[104]

6.10. Humins polymers with tunable flexibility

The addition of polymers to humins has been investigated to form humins-based copolymers. First, Licsandru and Mija reported the preparation of recyclable, humins-based copolymers consisting of industrial humins, epoxidized linseed oil (ELO), and Capcure® as a hardener.[117] It was possible to prepare resins with a bio-based carbon content up to 70 wt%, including up to 60 wt% humins. These resins showed thermomechanical reprocessability and high tunability of mechanical properties, ranging between rigid to elastomeric-like behaviour. Dinu and Mija[104] also reported the ability of humins to produce thermosets with a ductile character by the copolymerisation of 55 wt% humins with 45 wt% epoxy-based aliphatic ethers, i.e. poly(ethylene glycol) diglycidyl ether or glycerol diglycidyl ether. The resulting materials also show elastomeric behaviour (Fig. 9), with an impressive tensile strain break at up to ~60% in the case of copolymerisation with poly(ethylene glycol diglycidyl ether). This is an effect of the copolymer aliphatic chain length, with longer chains giving a stronger elastomeric effect, highlighting the possibility of tailoring the resin properties based on the application by selecting the composition. The mechanism of copolymerisation between humins and the aliphatic bis-epoxides using N,N-dimethylbenzylamine as promotor was investigated using Fourier transform infrared spectroscopy (FT-IR) and one dimensional (1D) and two-dimensional (2D) NMR spectroscopy. Using these techniques, the principal chain connections were identified.[107] Starting from this study, the same group also reported the preparation of composites between humins resins and industrial wastes (lignin and chicken feather powder).[279] Up to 10 wt% of these bio-fillers were incorporated into the humins matrix and the resulting composites were characterised by SEM, tensile tests, dynamic mechanical analysis (DMA), TGA, and water adsorption tests. Interestingly, while the Young's modulus values of the elastic humins matrix was estimated to be 1 MPa, it increased to 22 MPa when composites were made with the bio-fillers. Even better results were found for the rigid humins matrix composition, where the Young's modulus goes from 106 MPa (when polymerised alone) to 443 MPa (with chicken feathers) and 667 MPa (with lignin). The Mija group also investigated the properties of thermosets synthesised from humins and a bio-based tri-epoxide (the triglycidyl ether of phloroglucinol).[118,119] High values of bio-based carbon content (BCC ~95%) of these humins-based copolymer resins were reached. The copolymerisation reactivity studies done by DSC

revealed a good enthalpy of reaction (270-365 J·g^{-1}), reaching the maximum reactivity around 106-148 °C (depending on the formulation). The designed materials show high performance, with values for elastic storage moduli (E') in the glassy region ≈3.7-5 GPa, glass transition values from 122 °C to 154 °C, and Shore hardness values of 82-85 Shore D confirming the stiffness of these materials. The thermogravimetric analyses of these materials revealed very good thermal stability, with an onset of thermal decomposition (T5%, corresponding to a mass loss of 5%) at 272-277 °C. Three humins/epoxy-based copolymer thermosets of 95% BCC were developed, with mechanical performance comparable to those of industrial thermoset materials used in the construction or automotive sectors. In a recent study, a broad set of transesterification reactions with humins were carried out using different polylactic acid (PLA) and polycaprolactone grades.[240] High-strength thermoplastic elastomers with different structures were prepared via one-pot reactions in dioxane followed by solution casting. For example, highly elastomeric humic materials were produced with 12% of the D-enantiomer of amorphous PLA. The humins-containing materials displayed superior mechanical performance compared to the virgin PLA.[240] The applications reported in this section show the impressive opportunities for humins in innovative materials preparation in compliance with green chemistry principles but also responding to the high demand for biobased products.[286–288]

6.11. Humins-based foams

The production of carbon aerogels based on the conversion of inexpensive and abundant precursors using environmentally friendly processes is currently a highly attractive area in materials chemistry. The group of Titirici has reviewed the latest developments in the rapidly developing field of carbonaceous aerogels prepared from biomass and biomass-derived precursors, highlighting innovative approaches to green, sustainable nanomaterial synthesis.[289] Humins have been widely used as substrates in the preparation of porous carbon materials.[95,106,290] The preparation of 100% humins-based, carbonaceous, macroporous foams was reported by Mija et al. using a single step process and without requiring any additives.[95,106,290] By heating industrial humins to a temperature higher than 180 °C it was possible to produce a solid, homogeneous, porous, cross-linked material without pre-treatment or further modification (Fig. 10). These humins foams have porosities and properties that can be tailored by adjusting the reaction parameters.[95,106,290,291] The mechanism of formation consists of a combination of chemical and physical phenomena including the release of volatiles and gases during heating (leading to pore formation) and thermally-induced auto-cross-linking (leading to polymerisation of the matrix) (Fig. 10).
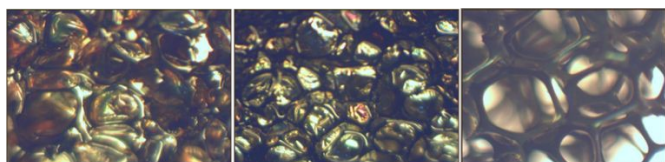
ARTICLE

Fig. 10. Optical microscopy photographs showing the morphologies of humins foams as a function of reaction temperatures (from left to right 220, 230 and 400°C).[95]
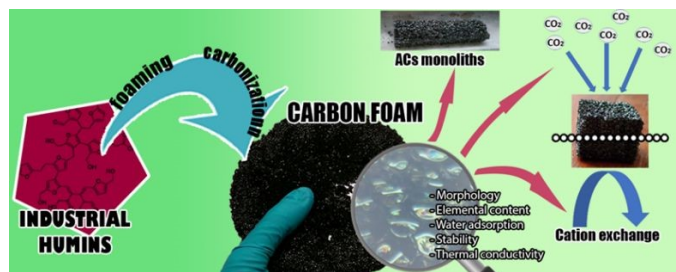

Fig. 11. Some examples of humins-derived foams and potential applications.[290]

By selecting the final temperature of preparation, it was possible to increase the carbon fraction of these materials up to 95%, creating a plethora of promising sustainable applications including electrodes for energy storage and conversion, as catalyst supports, or as cheap adsorbents (Fig. 11).[287] These humins foams were carbonized and activated using CO_2 to prepare activated carbon monoliths with surface areas up to 1482 m^2 g^{-1} that can compete with commercially available materials. These carbon monoliths have the advantage of a great adaptability, being easier to handle and recover. Moreover, the humins foams were able to sequester 3.66 wt% of CO_2 at 25 °C when carbonized at 700 °C, with the saturation reached after 44 min of treatment.[287] Other applications include the sequestration of dyes, which may be of value in water purification applications.[292,293] Furthermore, the higher thermal stability of humins foams compared to untreated humins should be emphasised, with no serious self-heating/self-ignition behaviour and relatively safe uses.[58]

Other bio-based materials were also produced by reacting the humins with tannins,[181,290,294–298] glycerol,[299] and chitosan.[300] As example, the combination of humins with various ratios of tannins/furfuryl alcohol results in self-blowing foams where humins contribute to the strength of the cell walls to give a predominantly interconnected cell structure. Humins have been shown to react well with condensed tannins, even at ambient temperature, but the reaction is slowed by their high viscosity compared to that of tannins with furfuryl alcohol.[139]

6.12. Humins as components of self-healing materials

The incorporation of humins into a Diels–Alder (DA) polymer network based on a furan-maleimide thermally-reversible cross-linking reaction was investigated by Cerdán et al.[301] The addition of humins led to the establishment of a considerable degree of self-healing capability which was observed by annealing the material for 1 h at 60 °C. However, this was achieved at the expense of a decline in mechanical properties, while the unmodified material showed no healing under the same conditions. The thermal healing step favoured irreversible

humins polycondensation, thus strengthening the material while maintaining the enhanced healing performance.[44] A synergistic healing mechanism was hypothesised based on the humins flowing towards the area of damage, followed by thermal humins cross-linking during the healing process, together with thermally-reversible DA bond recombination. A multi-material, soft robotic gripper was manufactured which not only showed improved recovery of functional performance upon healing but also tuneable stiffness by means of thermal cross-linking of the humins. For the first time, both damage healing and zone reinforcement for further damage prevention were achieved in a single, intrinsic, self-healing system.[301]

6.13. Humins in the production of electrically conductive materials

Humins chemically modified with succinic anhydride have shown the ability to be electrically conductive when cross-linked in the solid state then heated to temperatures from 250 °C up to 450 °C. These succinate-modified humins also showed ability to function in solution as photosensitizers in dye-sensitized solar cells.[235] Their area of applications can therefore be expanded to printing electronic circuits, organic light emitting diodes, actuators, electrodes, electromagnetic shielding, and microwave-absorbent coatings.[235] Novel nanocomposite materials have been prepared following a microwave-assisted method involving the reaction of sucrose with 2:1 phyllosilicate clay minerals. In this way, macromolecular intercalation materials (referred to by the authors as "caramel-clay nanocomposites") are formed when sucrose is heated with Na-montmorillonite in a microwave reactor. It would be interesting to evaluate if, under the applied experimental conditions, similar properties can be achieved when starting from industrial humins instead of sucrose. The most interesting feature of the synthesised caramel-clay compounds is their behaviour as precursors for carbon-clay nanocomposites. These nanocomposites are environmentally friendly, low-cost porous materials possessing electrical conductivity.[302,303] Silva et al.[304] showed the potential of humins in the production of carbon-based O_2 electrodes for Li-O_2 batteries. Such an application has potential because of the increasing need for the development of new, cost-competitive energy storage technologies with enhanced specific capacity compared to current state-of-the-art lithium-ion batteries. Humins were thermally treated under an inert atmosphere to enhance their electronic conductivity. The product was then mixed with a binder and spread out over a stainless-steel mesh to produce an O_2 electrode. It is anticipated that reactive industrial humins can also play a role as binders. Results of discharge experiments has demonstrated the potential of humins in the manufacture of carbon-based electrodes for batteries.[304]

6.14. Humins as photoactive products

Another application as UV-shielding materials was explored by blending humins with poly(vinyl alcohol) (PVA).[305] PVA-humins composite films showed high stability and durability even under extreme conditions, such as intense UV irradiation, sunlight

Green Chemistry Accepted Manuscript

exposure, and thermal treatment, while retaining their UV-shielding efficiency. PVA-humins (0.5–2.0 wt%) composite films showed 63-99% UV-shielding capacity across the entire UV range with 48-89% optical transparency. Decolorised humins composite films showed superior UV-shielding efficiency (98%) with >98% optical transparency. The thermal stability of the PVA-humin based films was a significant improvement over PVA films themselves, exhibiting a higher thermal degradation temperature (Td, by 57 °C) and glass transition temperature (by 7.3 °C). Furthermore, the composite film exhibited an excellent mechanical strength of 71 MPa and 338% strain to break compared to the neat PVA film (25 MPa mechanical strength and 177 % strain), along with an enhanced DMA storage modulus. UV shielding was demonstrated by a rhodamine B photodegradation stability, which showed that incorporation of humins resulted in only 0.4% degradation of rhodamine B, while unmodified PVA films showed 100% degradation. The enhanced photostability of rhodamine B while using PVA-humins was attributed to the formation of charge-transfer complexes between humins and PVA.[305] Tzvetkov *et al.*[306] demonstrated a facile ball milling approach to making photocatalytic humins derived from H_2SO_4-dehydrated glucose-fructose syrup. The photocatalytic performance was evaluated by monitoring the degradation of malachite green as a model pollutant under visible light irradiation, which showed that prolonged milling (up to 120 min) enhanced photocatalytic activity. The textural characteristics, adsorption capacity, and the presence of oxygen and sulphur functionalities in the humins were mainly responsible for the successful preparation of an efficient bio-based photocatalyst by ball milling.[306] A recent patent discloses a biodegradable biopolymer composition produced by mixing humins and chitosan and describes a method to prepare a UV-absorbing film wherein the humins were made by acid-catalysed dehydration of non-edible bio-waste materials.[307] Another patent discloses the use of humins as a component of electromagnetic wave absorbing functional materials. The preparation method comprises taking xylose-based humins as a carbon source, reacting them with cobalt-acetate and thiourea, and calcining the Co_9S_8 coated humins at different temperatures to obtain a composite material with a Co_9S_8/humins carbon core-shell structure that has excellent electromagnetic wave absorbing capacity in the frequency range of 2-18 GHz.[308]

7. Safety assessments and end of life of humins

Before humins can become a major component in a wide range of applications, thorough knowledge is needed of their potential toxicity and the safety both of the starting humin material as well as in the developed applications. In terms of ecological safety, thermal stability, and flammability of humins, a preliminary attempt at classification was conducted in 2018.[58] This work showed that the overall fire risk associated with humins is not significantly different from that of conventional woody materials. Further ecotoxicity and biodegradability tests

according to European regulations on the Registration, Evaluation, Authorisation and Restriction of Chemicals (REACH), along with primary evaluation of aquatic ecosystem hazards, were published in 2019.[285] It is well known that furan-based materials have flame retardant properties. For example, a flame-retardant material derived from a furan resin and basalt fibre was prepared which was suitable for use in interior applications.[309] Wang and Dong[310] reviewed various furan-based polymers with good flame-retardant properties. A modification of the furan-based materials with phosphor containing compounds further improves the flame resistance. However, the flame-retardant properties of fully furan-based resins are usually limited.[310]

To our knowledge, the work of Muralidhara *et al.* was the first published information about humins and humins-based foams focusing on safety issues, which is often an underappreciated aspect of the sustainable use of new biobased feedstocks and materials.[58] However, it was stated that further work is still needed to achieve a more comprehensive insight and understanding of safety pertaining to use of humins and humins-based derivatives.[58] The further processing of humins in different applications will likely alter the safety aspects of these end products, which is a matter for future studies.[58,285]

8. Conclusions and outlook

Humins are side products of the acid-catalysed dehydration of sugars and other carbohydrates into furanic building blocks as well as levulinic acid. In the previous century, research was mainly focused on attempts to avoid/minimize the formation of humins based only on lab-scale reactions. However, it is now generally accepted that under commercially relevant conditions the formation of humins is unavoidable. The main challenges around humins are understanding their formation mechanism and the evaluation of the parameters that lead to their production (e.g. type of feedstock, catalysts, solvents, pH, temperature, reaction time, combined severity, substrate loading, reactor configuration) in order to increase the yields of the primary products at the expense of humins generation. Much in the way of fundamental information on humins formation and composition has emerged, but the picture is far from complete. The high dependence on the feedstock and process parameters used during industrial humins production leads to dissimilarities between a wide variety of samples reported in literature. More work is needed on the molecular mass determination of (soluble) humins, reactions occurring during the processing and storage of reactive humins, and knowledge on how the properties of the humins can be modified to make them better suitable as feedstocks for specific higher-value applications.

During the last decade, interest has indeed shifted to some extent from avoidance of humins formation towards valorisation of this side-stream. Therefore, industrial humins are attracting more and more attention as feedstock for a wide range of applications. Much work is now being devoted to the deliberate synthesis of humins and hydrothermal carbons from a variety of sources. Many studies have demonstrated practical

Journal Name

ARTICLE

valorisation routes for these products, with applications including the production of chemicals and fuels, polymers and composites, carbon-based porous materials and activated carbons, catalysts and catalyst support materials, self-healing materials, wood and fibre composites, and impregnating agents for wood.

With the construction of Origin Material's CMF production facility and the startup of Avantium's commercial FDCA plant, multi-ton quantities of industrial humins will soon become available. Improvement of the business value proposition for such humins is therefore a necessity for a truly circular, biobased economy.

Author Contributions

Conceptualisation, P.T. and E.d.J.; writing—original draft preparation, E.d.J., P.T., S.C.; writing—review and editing, E.d.J., S.C., M.M., T.C., A.M.; visualisation, P.T., S.C.; supervision A.M., M.M., E.d.J.; funding acquisition, E.d.J., A.M.

All authors have read and agreed to the published version of the manuscript.

Conflicts of Interest

The authors declare no conflict of interest.

Acknowledgments

References

1   J. E. Cohen, *Science (1979)*, 2003, **302**, 1172–1175.

2   G. Resch, A. Held, T. Faber, C. Panzer, F. Toro and R. Haas, *Energy Policy*, 2008, **36**, 4048–4056.

3   D. Lin, L. Wambersie and M. Wackernagel, *Estimating the Date of Earth Overshoot Day 2021*, 2021.

4   D. Gale, *The Theory of Linear Economic Models*, The University of Chicago Press, Chicago, 1989.

5   P. Ghisellini, C. Cialani and S. Ulgiati, *J Clean Prod*, 2016, **114**, 11–32.

6   M. Carus, L. Dammer, A. Raschka, P. Skoczinski and C. vom Berg, Renewable Carbon – Key to a Sustainable and Future-Oriented Chemical and Plastic Industry, https://renewable-carbon.eu/publications/product/nova-paper-12-renewable-carbon-key-to-a-sustainable-and-future-oriented-chemical-and-plastic-industry-%E2%88%92-full-version/, (accessed 7 February 2025).

7   P. Krugman, *Oxf Rev Econ Policy*, 1998, **14**, 7–17.

8   E. de Jong, A. Higson, P. Walsh and M. Wellisch, *Biofuels, Bioproducts and Biorefining*, 2012, **6**, 606–624.

9   E. de Jong, H. Stichnothe, G. Bell and H. Jørgensen, Bio-Based Chemicals A 2020 Update., https://www.ieabioenergy.com/blog/publications/new-publication-bio-based-chemicals-a-2020-update/, (accessed 7 February 2025).

10   A. Muscat, E. M. de Olde, I. J. M. de Boer and R. Ripoll-Bosch, *Glob Food Sec*, 2020, **25**, 100330.

11   M. Carus, O. Porc, C. vom Berg, M. Kempen, F. Schier and J. Tandetzki, Is there Enough Biomass to Defossilise the Chemicals and Derived Materials Sector by 2050? – A Joint BIC and RCI

Scientific Background Report, https://renewable-carbon.eu/publications/product/is-there-enough-biomass-to-defossilise-the-chemicals-and-derived-materials-sector-by-2050-a-joint-bic-and-rci-scientific-background-report/, (accessed 7 February 2025).

12   N. Mosier, C. Wyman, B. Dale, R. Elander, Y. Y. Lee, M. Holtzapple and M. Ladisch, *Bioresour Technol*, 2005, **96**, 673–686.

13   E. de Jong and R. J. A. Gosselink, in *Bioenergy Research: Advances and Applications*, eds. V. K. Gupta, M. G. Tuohy, C. P. Kubicek, J. Saddler and F. Xu, Elsevier, Amsterdam, 2014, pp. 277–313.

14   J. Pérez, J. Muñoz-Dorado, T. de la Rubia and J. Martínez, *International Microbiology*, 2002, **5**, 53–63.

15   D. J. Hayes, S. Fitzpatrick, M. H. B. Hayes and J. R. H. Ross, in *Biorefineries-Industrial Processes and Products*, eds. B. Kamm, P. R. Gruber and M. Kamm, 2005, pp. 139–164.

16   R. Rinaldi, R. Palkovits and F. Schüth, *Angewandte Chemie International Edition*, 2008, **47**, 8047–8050.

17   X.-J. Ji, H. Huang, Z.-K. Nie, L. Qu, Q. Xu and G. T. Tsao, in *Biotechnology in China III: Biofuels and Bioenergy*, eds. F.-W. Bai, C.-G. Liu, H. Huang and G. T. Tsao, Springer Berlin Heidelberg, Berlin, Heidelberg, 2012, pp. 199–224.

18   B. Girisuta, B. Danon, R. Manurung, L. P. B. M. Janssen and H. J. Heeres, *Bioresour Technol*, 2008, **99**, 8367–8375.

19   R. J. Van Putten, J. C. Van Der Waal, E. De Jong, C. B. Rasrendra, H. J. Heeres and J. G. De Vries, *Chem Rev*, 2013, **113**, 1499–1597.

20   B. Velaga and N. R. Peela, *Green Chemistry*, 2022, **24**, 3326–3343.

21   G. R. Gomes, D. S. Rampon and L. P. Ramos, *Appl Catal A Gen*, 2017, **545**, 127–133.

22   G. Tsilomelekis, M. J. Orella, Z. Lin, Z. Cheng, W. Zheng, V. Nikolakis and D. G. Vlachos, *Green Chem.*, 2016, **18**, 1983–1993.

23   G. Portillo Perez, A. Mukherjee and M.-J. Dumont, *Journal of Industrial and Engineering Chemistry*, 2019, **70**, 1–34.

24   F. Menegazzo, E. Ghedini and M. Signoretto, *Molecules*, 2018, **23**, 2201.

25   R.-J. van Putten, J. N. M. Soetedjo, E. A. Pidko, J. C. van der Waal, E. J. M. Hensen, E. de Jong and H. J. Heeres, *ChemSusChem*, 2013, **6**, 1681–1687.

26   R.-J. van Putten, J. C. van der Waal, M. Harmse, H. H. van de Bovenkamp, E. de Jong and H. J. Heeres, *ChemSusChem*, 2016, **9**, 1827–1834.

27   R.-J. van Putten, A. S. Dias and E. de Jong, in *Catalytic Process Development for Renewable Materials*, eds. P. Imhof and J. C. van des Waal, 2013, pp. 81–117.

28   B. Girisuta, University of Groningen, 2007.

29   V. Isoni, D. Kumbang, P. N. Sharratt and H. H. Khoo, *J Environ Manage*, 2018, **214**, 267–275.

30   Y. Shen, J. Sun, B. Wang, F. Xu and R. Sun, in *Biomass as Renewable Raw Material to Obtain Bioproducts of High-Tech Value*, eds. V. Popa and I. Volf, Elsevier, 2018, pp. 235–269.

31   Y. Román-Leshkov, C. J. Barrett, Z. Y. Liu and J. A. Dumesic, *Nature*, 2007, **447**, 982–985.

32   C. Moreau, in *Catalysts for Fine Chemical Synthesis*, 2006, pp. 141–156.

33   M. E. Zakrzewska, E. Bogel-Łukasik and R. Bogel-Łukasik, *Chem Rev*, 2011, **111**, 397–417.

34   J. C. van der Waal and E. de Jong, in *Industrial Biorenewables*, 2016, pp. 97–120.

35   B. F. M. Kuster, *Starch - Stärke*, 1990, **42**, 314–321.

36   R.-J. van Putten, J. G. M. Winkelman, F. Keihan, J. C. van der Waal, E. de Jong and H. J. Heeres, *Ind Eng Chem Res*, 2014, **53**, 8285–8290.

37   V. Choudhary, S. H. Mushrif, C. Ho, A. Anderko, V. Nikolakis, N. S. Marinkovic, A. I. Frenkel, S. I. Sandler and D. G. Vlachos, *J Am Chem Soc*, 2013, **135**, 3997–4006.

38   W. Deng, Q. Zhang and Y. Wang, *Sci China Chem*, 2015, **58**, 29–46.

39   A. Mukherjee, M. J. Dumont and V. Raghavan, *Biomass Bioenergy*, 2015, **72**, 143–183.

40   G. J. Mulder, *Journal für Praktische Chemie*, 1840, **21**, 321–370.

41   L. Yu, N. Brun, K. Sakaushi, J. Eckert and M. M. Titirici, *Carbon N Y*, 2013, **61**, 245–253.

42   B. V Timokhin, V. A. Baransky and G. D. Eliseeva, *Russian Chemical Reviews*, 1999, **68**, 73–84.

43   R. H. Leonard, *Ind Eng Chem*, 1956, **48**, 1330–1341.

44   M. Sasaki, T. Adschiri and K. Arai, *J Agric Food Chem*, 2003, **51**, 5376–5381.

45   J. J. Bozell, L. Moens, D. C. Elliott, Y. Wang, G. G. Neuenscwander, S. W. Fitzpatrick, R. J. Bilski and J. L. Jarnefeld, *Resour Conserv Recycl*, 2000, **28**, 227–239.

46   V. Ghorpade and M. Hanna, in *Cereals: Novel Uses and Processes*, eds. G. M. Campbell, C. Webb and S. L. McKee, Springer US, Boston, MA, 1997, pp. 49–55.

47   X. Cao, J. Wei, H. Liu, X. Lv, X. Tang, X. Zeng, Y. Sun, T. Lei, S. Liu and L. Lin, *Journal of Chemical Technology & Biotechnology*, 2019, **94**, 167–177.

48   S. Constant, C. S. Lancefield, W. Vogelzang, R. K. Pazhavelikkakath Purushothaman, A. E. Frissen, K. Houben, P. de Peinder, M. Baldus, B. M. Weckhuysen, D. S. van Es and P. C. A. Bruijnincx, *Green Chemistry*, 2024, **26**, 7739–7751.

49   A. F. Sousa, C. Vilela, A. C. Fonseca, M. Matos, C. S. R. Freire, G.-J. M. Gruter, J. F. J. Coelho and A. J. D. Silvestre, *Polym Chem*, 2015, **6**, 5961–5983.

50   A. C. Cardiel, B. J. Taitt and K.-S. Choi, *ACS Sustain Chem Eng*, 2019, **7**, 11138–11149.

51   R. Ooms, M. Dusselier, J. A. Geboers, B. Op de Beeck, R. Verhaeven, E. Gobechiya, J. A. Martens, A. Redl and B. F. Sels, *Green Chemistry*, 2014, **16**, 695–707.

52   E. de Jong, M. A. Dam, L. Sipos and G.-J. M. Gruter, in *Biobased Monomers, Polymers, and Materials*, eds. P. B. Smith and R. Gross, American Chemical Society, 2012, vol. 1105, pp. 1–13.

53   E. de Jong, H. A. Visser, A. S. Dias, C. Harvey and G.-J. M. Gruter, *Polymers (Basel)*, 2022, **14**, 943.

54   A. J. J. E. Eerhart, A. P. C. Faaij and M. K. Patel, *Energy Environ Sci*, 2012, **5**, 6407–6422.

55   D. W. Rackemann and W. O. S. Doherty, *Biofuels, Bioproducts and Biorefining*, 2011, **5**, 198–214.

56   T. Wang, M. W. Nolte and B. H. Shanks, *Green Chemistry*, 2014, **16**, 548–572.

57   C. Sievers, I. Musin, T. Marzialetti, M. B. Valenzuela Olarte, P. K. Agrawal and C. W. Jones, *ChemSusChem*, 2009, **2**, 665–671.

58   A. Muralidhara, P. Tosi, A. Mija, N. Sbirrazzuoli, C. Len, V. Engelen, E. de Jong and G. Marlair, *ACS Sustain Chem Eng*, 2018, **6**, 16692–16701.

59   M. Mascal, *ChemSusChem*, 2015, **8**, 3391–3395.

60   M. Mascal, *ACS Sustain Chem Eng*, 2019, **7**, 5588–5601.

61   Origin Materials Announces Startup of Origin 1, World's First Commercial CMF Plant, https://investors.originmaterials.com/news-releases/news-release-details/origin-materials-announces-startup-origin-1-worlds-first, (accessed 7 February 2025).

62   J. Bueno Moron, G. van Klink and G.-J. M. Gruter, *ACS Sustain Chem Eng*, 2023, **11**, 17492–17509.

63   J. Bueno Morón, F. Arbore, G. P. M. van Klink, M. Mascal and G.-J. M. Gruter, *ChemSusChem*, 2024, **17**, e202400495.

64   J. Bueno Moron, G. P. M. van Klink and G.-J. M. Gruter, *Waste Management Bulletin*, 2024, **2**, 58–68.

65   N. Leenders, R. M. Moerbeek, M. J. Puijk, R. J. A. Bronkhorst, J. Bueno Morón, G. P. M. van Klink and G.-J. M. Gruter, *Nat Commun*, 2025, **16**, 738.

66   M. Mascal and E. B. Nikitin, *Green Chem.*, 2010, **12**, 370–373.

67   S. Karimi, S. Gharouni Fattah, Z. Li, M. Zuo, M. Nasrollahzadeh and X. Zeng, *Green Chemistry*, 2025, **27**, 379–402.

68   A. F. V Grote and B. Tollens, *Justus Liebigs Ann Chem*, 1875, **175**, 181–204.

69   A. F. V Grote and B. Tollens, *Justus Liebigs Ann Chem*, 1881, **206**, 226–232.

70   A. Schweizer, *Recueil des Travaux Chimiques des Pays-Bas*, 1938, **57**, 886–890.

71   A. Schweizer, *Recueil des Travaux Chimiques des Pays-Bas*, 1940, **59**, 781–784.

72   J. J. Blanksma and G. Egmond, *Recueil des Travaux Chimiques des Pays-Bas*, 1946, **65**, 309–310.

73   I. V. Sumerskii, S. M. Krutov and M. Ya. Zarubin, *Russian Journal of Applied Chemistry*, 2010, **83**, 320–327.

74   C. Chang, X. Ma and P. Cen, *Chin J Chem Eng*, 2006, **14**, 708–712.

75   A. Ukalska-Jaruga, A. Klimkowicz-Pawlas and B. Smreczak, *Soil Use Manag*, 2019, **35**, 595–606.

76   D. Zhang, H. Dang, Z. Li and C. Zhang, *Environmental Pollution*, 2019, **252**, 296–304.

77   E. H. Novotny, M. H. B. Hayes, E. R. de Azevêdo and T. J. Bonagamba, in *International Agrichar Initiative - IAI Conference*, International Agrichar Initiative - IAI, 2007.

78   M. H. B. Hayes, R. Mylotte and R. S. Swift, in *Advances in Agronomy*, ed. D. L. Sparks, Academic Press, 2017, vol. 143, pp. 47–138.

79   S. Sutradhar and P. Fatehi, *Biotechnology for Biofuels and Bioproducts*, 2023, **16**, 38.

80   B. Girisuta, L. P. B. M. Janssen and H. J. Heeres, *Green Chemistry*, 2006, **8**, 701–709.

81   B. Girisuta, L. P. B. M. Janssen and H. J. Heeres, *Ind Eng Chem Res*, 2007, **46**, 1696–1708.

82   K. D. Baugh and P. L. McCarty, *Biotechnol Bioeng*, 1988, **31**, 50–61.

83   G. C. A. Luijkx, F. van Rantwijk and H. van Bekkum, *Carbohydr Res*, 1993, **242**, 131–139.

84   Li Liu, *Biomass-Derived Humins*, Springer , Singapore, 2023.

85   IFPEN and ResiCare, leaders in the development of a production process for the non-toxic* biobased molecule 5-HMF, https://www.resicare.com/news/ifpen-and-resicare-leaders-in-the-development-of-a-

production-process-for-the-non-toxic-biobased-molecule-5-hmf/, (accessed 7 February 2025).

86   US Pat., US 2015/0203462 A1, 2015.

87   H. E. Hoydonckx, W. M. Van Rhijn, W. Van Rhijn, D. E. De Vos and P. A. Jacobs, in *Ullmann's Encyclopedia of Industrial Chemistry*, 2007.

88   WO Pat, WO2000/047569 A1, 2000.

89   A. Schweizer, *Recueil des Travaux Chimiques des Pays-Bas*, 1938, **57**, 345–382.

90   G. Sengar and H. K. Sharma, *J Food Sci Technol*, 2014, **51**, 1686–1696.

91   R. Weingarten, J. Cho, R. Xing, W. C. Conner Jr and G. W. Huber, *ChemSusChem*, 2012, **5**, 1280–1290.

92   R. Weingarten, J. Cho, Jr. Conner Wm. Curtis and G. W. Huber, *Green Chemistry*, 2010, **12**, 1423–1429.

93   S. Agarwal, D. van Es and H. J. Heeres, *J Anal Appl Pyrolysis*, 2017, **123**, 134–143.

94   Z. Lin, M. Ierapetritou and V. Nikolakis, *AIChE Journal*, 2013, **59**, 2079–2087.

95   WO Pat., WO 2017/074183 A1, 2017.

96   EU Pat., EP3519480B1, 2017.

97   J. Horvat, B. Klaić, B. Metelko and V. Šunjić, *Croatica Chemica Acta*, 1986, **59**, 429–438.

98   R. Choowang, J. Lin and G. Zhao, *Bioresources*, 2019, **14**, 943–953.

99   P. Yazdani, B. Wang, S. Rimaz, S. Kawi and A. Borgna, *Molecular Catalysis*, 2019, **466**, 138–145.

100   J. Pang, M. Zheng, X. Li, Y. Jiang, Y. Zhao, A. Wang, J. Wang, X. Wang and T. Zhang, *Appl Catal B*, 2018, **239**, 300–308.

101   C. Li, G. Xu, C. Wang, L. Ma, Y. Qiao, Y. Zhang and Y. Fu, *Green Chemistry*, 2019, **21**, 2234–2239.

102   I. van Zandvoort, E. J. Koers, M. Weingarth, P. C. A. Bruijnincx, M. Baldus and B. M. Weckhuysen, *Green Chem.*, 2015, **17**, 4383–4392.

103   I. van Zandvoort, Y. Wang, C. B. Rasrendra, E. R. H. van Eck, P. C. A. Bruijnincx, H. J. Heeres and B. M. Weckhuysen, *ChemSusChem*, 2013, **6**, 1745–58.

104   R. Dinu and A. Mija, *Green Chemistry*, 2019, **21**, 6277–6289.

105   M. Sevilla and M. Titirici, *Bol Grupo Español Carbón*, 2012, **25**, 7–17.

106   P. Tosi, G. P. M. van Klink, A. Celzard, V. Fierro, L. Vincent, E. de Jong and A. Mija, *ChemSusChem*, 2018, **11**, 2797–2809.

107   X. Montané, R. Dinu and A. Mija, *Molecules*, 2019, **24**, 4110.

108   S. K. R. Patil and C. R. F. Lund, *Energy & Fuels*, 2011, **25**, 4745–4755.

109   I. Van Zandvoort, E. R. H. Van Eck, P. De Peinder, H. J. Heeres, P. C. A. Bruijnincx and B. M. Weckhuysen, *ACS Sustain Chem Eng*, 2015, **3**, 533–543.

110   I. van Zandvoort, University of Utrecht, 2015.

111   J.-M. Pin, N. Guigo, A. Mija, L. Vincent, N. Sbirrazzuoli, J. C. van der Waal and E. de Jong, *ACS Sustain Chem Eng*, 2014, **2**, 2182–2190.

112   WO Pat., WO2015/088341 A1, 2015.

113   A. Mija, J. C. van der Waal, J. M. Pin, N. Guigo and E. de Jong, *Constr Build Mater*, 2017, **139**, 594–601.

114   A. Sangregorio, N. Guigo, J. C. van der Waal and N. Sbirrazzuoli, *Compos Sci Technol*, 2019, **171**, 70–77.

ARTICLE

115   A. Sangregorio, N. Guigo, J. C. van der Waal and N. Sbirrazzuoli, *ChemSusChem*, 2018, **11**, 4246–4255.

116   A. Sangregorio, A. Muralidhara, N. Guigo, G. Marlair, E. de Jong and N. Sbirrazzuoli, *Composites Part C: Open Access*, 2021, **4**, 100109.

117   E. Licsandru and A. Mija, *Cellulose Chemistry and Technology*, 2019, **53**, 963–969.

118   C. Cantarutti, R. Dinu and A. Mija, *Biomacromolecules*, 2020, **21**, 517–533.

119   R. Dinu and A. Mija, *J. Mat. Sci. Res.*, 2020, **9**, 1.

120   E. Licsandru, M. Gaysinski and A. Mija, *Polymers (Basel)*, 2020, **12**, 1583.

121   N. Shi, Q. Liu, R. Ju, X. He, Y. Zhang, S. Tang and L. Ma, *ACS Omega*, 2019, **4**, 7330–7343.

122   N. Shi, Q. Liu, H. Cen, R. Ju, X. He and L. Ma, *Biomass Convers Biorefin*, 2020, **10**, 277–287.

123   P. P. Thoresen, H. Lange, U. Rova, P. Christakopoulos and L. Matsakas, *Int J Biol Macromol*, 2023, **233**, 123471.

124   Z. Cheng, K. A. Goulas, N. Quiroz Rodriguez, B. Saha and D. G. Vlachos, *Green Chem.*, 2020, **22**, 2301–2309.

125   S. K. R. Patil, J. Heltzel and C. R. F. Lund, *Energy & Fuels*, 2012, **26**, 5281–5293.

126   S. Constant, C. S. Lancefield, B. M. Weckhuysen and P. C. A. Bruijnincx, *ACS Sustain Chem Eng*, 2016, **1**, 965–972.

127   N. Baccile, C. Falco and M. M. Titirici, *Green Chem.*, 2014, **16**, 4839–4869.

128   A. Wassenberg, T. Esser, M. J. Poller and J. Albert, *Materials*, 2023, **16**, 2864.

129   S. Liu, Y. Zhu, Y. Liao, H. Wang, Q. Liu, L. Ma and C. Wang, *Appl. Energy Combust. Sci.*, 2022, **10**, 100062.

130   H. Shen, H. Shan and L. Liu, *ChemSusChem*, 2020, **13**, 513–519.

131   B. Cheng, X. Wang, Q. Lin, X. Zhang, L. Meng, R.-C. Sun, F. Xin and J. Ren, *J Agric Food Chem*, 2018, **66**, 11981–11989.

132   C. B. Rasrendra, M. Windt, Y. Wang, S. Adisasmito, I. G. B. N. Makertihartha, E. R. H. van Eck, D. Meier and H. J. Heeres, *J Anal Appl Pyrolysis*, 2013, **104**, 299–307.

133   M. Sevilla and A. B. Fuertes, *Carbon N Y*, 2009, **47**, 2281–2289.

134   M. Sevilla and A. B. Fuertes, *Chemistry - A European Journal*, 2009, **15**, 4195–4203.

135   T. M. C. Hoang, B. Geerdink, J. M. Sturm, L. Lefferts and K. Seshan, *Appl Catal B*, 2015, **163**, 74–82.

136   Rattana C., Jian L. and Guang J.Z., *Bioresources*, 2018, **14**, 943–953.

137   J. Horvat, B. Klaić, B. Metelko and V. Šunjić, *Tetrahedron Lett*, 1985, **26**, 2111–2114.

138   Z. Cheng, J. L. Everhart, G. Tsilomelekis, V. Nikolakis, B. Saha and D. G. Vlachos, *Green Chem.*, 2018, **20**, 997–1006.

139   X. Chen, N. Guigo, A. Pizzi, N. Sbirrazzuoli, B. Li, E. Fredon and C. Gerardin, *Polymers*, 2020, **12**, 2732.

140   Z. Xu, Y. Yang, P. Yan, Z. Xia, X. Liu and Z. C. Zhang, *RSC Adv*, 2020, **10**, 34732–34737.

141   B. Velaga, R. P. Parde, J. Soni and N. R. Peela, *Microporous and Mesoporous Materials*, 2019, **287**, 18–28.

142   A. Sangregorio, N. Guigo, E. de Jong and N. Sbirrazzuoli, *Polymers*, 2019, **11**, 1804.

Green Chemistry Accepted Manuscript

143   X. Fu, Y. Hu, Y. Zhang, Y. Zhang, D. Tang, L. Zhu and C. Hu, *ChemSusChem*, 2020, **13**, 501–512.

144   A. Sangregorio, A. Muralidhara, N. Guigo, L. G. Thygesen, G. Marlair, C. Angelici, E. de Jong and N. Sbirrazzuoli, *Green Chem.*, 2020, **22**, 2786–2798.

145   S. J. Dee and A. T. Bell, *ChemSusChem*, 2011, **4**, 1166–1173.

146   L. Filiciotto, A. M. Balu, A. A. Romero, C. Angelici, J. C. van der Waal and R. Luque, *Molecular Catalysis*, 2019, **479**, 110564.

147   M. M. Titirici, M. Antonietti and N. Baccile, *Green Chemistry*, 2008, **10**, 1204–1212.

148   X. Sun and Y. Li, *Angewandte Chemie International Edition*, 2004, **43**, 597–601.

149   Y. Mi, W. Hu, Y. Dan and Y. Liu, *Mater Lett*, 2008, **62**, 1194–1196.

150   M. M. Titirici, R. J. White, C. Falco and M. Sevilla, *Energy Environ Sci*, 2012, **5**, 6796–6822.

151   C. Yao, Y. Shin, L.-Q. Wang, C. F. Windisch, W. D. Samuels, B. W. Arey, C. Wang, W. M. Risen and G. J. Exarhos, *J. Phys. Chem. C*, 2007, **111**, 15141–15145.

152   J. Ryu, Y.-W. Suh, D. J. Suh and D. J. Ahn, *Carbon*, 2010, **48**, 1990–1998.

153   A. Chuntanapum and Y. Matsumura, *Ind. Eng Chem. Res.*, 2009, **48**, 9837–9846.

154   N. Baccile, G. Laurent, F. Babonneau, F. Fayon, M.-M. Titirici and M. Antonietti, *The Journal of Physical Chemistry C*, 2009, **113**, 9644–9654.

155   V. Maruani, S. Narayanin-Richenapin, E. Framery and B. Andrioletti, *ACS Sustain Chem Eng*, 2018, **6**, 13487–13493.

156   C. Falco, N. Baccile and M.-M. Titirici, *Green Chemistry*, 2011, **13**, 3273–3281.

157   S. Crossley, J. Faria, M. Shen and D. E. Resasco, *Science (1979)*, 2010, **327**, 68–72.

158   G. W. Huber, J. N. Chheda, C. J. Barrett and J. A. Dumesic, *Science (1979)*, 2005, **308**, 1446–1450.

159   C. L. Williams, C.-C. Chang, P. Do, N. Nikbin, S. Caratzoulas, D. G. Vlachos, R. F. Lobo, W. Fan and P. J. Dauenhauer, *ACS Catal*, 2012, **2**, 935–939.

160   S. Liu, K. Wang, H. Yu, B. Li and S. Yu, *Sci Rep*, 2019, **9**, 1810.

161   S. Liu, X. Cheng, S. Sun, Y. Chen, B. Bian, Y. Liu, L. Tong, H. Yu, Y. Ni and S. Yu, *ACS Omega*, 2021, **6**, 15940–15947.

162   B. Girisuta, L. P. B. M. Janssen and H. J. Heeres, *Chemical Engineering Research and Design*, 2006, **84**, 339–349.

163   C. Moreau, R. Durand, S. Razigade, J. Duhamet, P. Faugeras, P. Rivalier, P. Ros and G. Avignon, *Appl Catal A Gen*, 1996, **145**, 211–224.

164   B. F. M. Kuster, *Carbohydr Res*, 1977, **54**, 177–183.

165   A. S. Amarasekara and A. Razzaq, *Carbohydr Res*, 2014, **386**, 86–91.

166   F. S. Asghari and H. Yoshida, *Ind Eng Chem Res*, 2007, **46**, 7703–7710.

167   M.-M. Titirici, R. J. White, N. Brun, V. L. Budarin, D. S. Su, F. del Monte, J. H. Clark and M. J. MacLachlan, *Chem Soc Rev*, 2015, **44**, 250–290.

168   J. Shen and C. E. Wyman, *AIChE Journal*, 2012, **58**, 236–246.

169   D. Jung, P. Körner and A. Kruse, *Biomass Convers Biorefin*, 2021, **11**, 1155–1170.

170   Y. Román-Leshkov, M. Moliner, J. A. Labinger and M. E. Davis, *Angewandte Chemie International Edition*, 2010, **49**, 8954–8957.

View Article Online
DOI: 10.1039/D4GC06244B

171 E. A. Pidko, V. Degirmenci and E. J. M. Hensen, *ChemCatChem*, 2012, **4**, 1263–1271.

172 P. Ramesh, A. Kritikos and G. Tsilomelekis, *React Chem Eng*, 2019, **4**, 273–277.

173 W. Guo, H. C. Bruining, H. J. Heeres and J. Yue, *Green Chemistry*, 2023, **25**, 5878–5898.

174 W. Mamo, Y. Chebude, C. Márquez-Álvarez, I. Díaz and E. Sastre, *Catal Sci Technol*, 2016, **6**, 2766–2774.

175 Y. Zuo, Y. Zhang and Y. Fu, *ChemCatChem*, 2014, **6**, 753–757.

176 D. Mercadier, L. Rigal, A. Gaset and J.-P. Gorrichon, *J. Chem. Technol. Biotechnol.,* 1981, **31**, 489–496.

177 L. Zhang, G. Xi, Z. Chen, Z. Qi and X. Wang, *Chem. Eng. J.*, 2017, **307**, 877–883.

178 S. Xu, D. Pan, Y. Wu, N. Xu, H. Yang, L. Gao, W. Li and G. Xiao, *Ind Eng Chem Res*, 2019, **58**, 9276–9285.

179 Y. Wang, Y. Huang, L. Liu, L. He, T. Li, C. Len and W. Yang, *ACS Sustain Chem Eng*, 2020, **8**, 14576–14583.

180 D. Garcés, L. Faba, E. Díaz and S. Ordóñez, *ChemSusChem*, 2019, **12**, 924–934.

181 Y. Hu, Y. Zhang, X. Fu, D. Tang, H. Li, P. Hu, L. Zhu and C. Hu, *Ind Eng Chem Res*, 2022, **61**, 5786–5796.

182 P. Hu, Y. Hu, H. Li, L. Li, Z. Xue, D. Wu, J. Zhao, C. Hu and L. Zhu, *Carbohydr Polym*, 2023, **309**, 120692.

183 Z. Cao, Z. Fan, Y. Chen, M. Li, T. Shen, C. Zhu and H. Ying, *Appl Catal B*, 2019, **244**, 170–177.

184 M. J. F. Costa, A. A. S. Gonçalves, R. Rinaldi, H. Bradtmüller, H. Eckert and E. B. Ferreira, *Catal Commun*, 2023, **174**, 106577.

185 L. Ricciardi, W. Verboom, J.-P. Lange and J. Huskens, *Sustain Energy Fuels*, 2022, **6**, 11–28.

186 R. M. Musau and R. M. Munavu, *Biomass*, 1987, **13**, 67–74.

187 C. Moreau, M. N. Belgacem and A. Gandini, *Top Catal*, 2004, **27**, 11–30.

188 M. R. Whitaker, A. Parulkar, P. Ranadive, R. Joshi and N. A. Brunelli, *ChemSusChem*, 2019, **12**, 2211–2219.

189 P. Maneechakr and S. Karnjanakom, *Research on Chemical Intermediates*, 2019, **45**, 743–756.

190 US2750394A, 1956.

191 US2917520A, 1957.

192 J. N. Chheda, Y. Román-Leshkov and J. A. Dumesic, *Green Chemistry*, 2007, **9**, 342–350.

193 B. F. M. Kuster and H. J. C. Der Van Steen, *Starch - Stärke*, 1977, **29**, 99–103.

194 L. Faba, D. Garcés, E. Díaz and S. Ordóñez, *ChemSusChem*, 2019, **12**, 3769–3777.

195 Q. Zhang, K. De Oliveira Vigier, S. Royer and F. Jérôme, *Chem Soc Rev*, 2012, **41**, 7108–7146.

196 K. D. O. Vigier, A. Benguerba, J. Barrault and F. Jérôme, *Green Chemistry*, 2012, **14**, 285–289.

197 F. Jérôme and K. De Oliveira Vigier, *Catalysts*, DOI:10.3390/catal7070218.

198 F. Liu, M. Audemar, K. De Oliveira Vigier, D. Cartigny, J.-M. Clacens, M. F. Costa Gomes, A. A. H. Pádua, F. De Campo and F. Jérôme, *Green Chemistry*, 2013, **15**, 3205–3213.

199 C. Ruan, H. J. Heeres and J. Yue, *J Flow Chem*, 2023, **13**, 155–168.

200 X. Fang, Z. Wang, B. Yuan, W. Song, S. Li and W. Lin, *ChemistrySelect*, 2018, **3**, 12243–12249.

201   G. Gómez Millán, S. Hellsten, A. W. T. King, J.-P. Pokki, J. Llorca and H. Sixta, *Journal of Industrial and Engineering Chemistry*, 2019, **72**, 354–363.

202   S. G. Wettstein, D. M. Alonso, Y. Chong and J. A. Dumesic, *Energy Environ Sci*, 2012, **5**, 8199–8203.

203   P. Chen, A. Yamaguchi, N. Hiyoshi and N. Mimura, *Fuel*, 2023, **334**, 126632.

204   C. Sievers, T. Marzialetti, T. J. C. Hoskins, M. B. Valenzuela Olarte, P. K. Agrawal and C. W. Jones, *Bioresour Technol*, 2009, **100**, 4758–4765.

205   C. Sievers, M. B. Valenzuela-Olarte, T. Marzialetti, I. Musin, P. K. Agrawal and C. W. Jones, *Ind Eng Chem Res*, 2009, **48**, 1277–1286.

206   H. Zhao, J. E. Holladay, H. Brown and Z. C. Zhang, *Science (1979)*, 2007, **316**, 1597–1600.

207   G. Yong, Y. Zhang and J. Y. Ying, *Angewandte Chemie International Edition*, 2008, **47**, 9345–9348.

208   M. Conrad and M. Guthzeit, *Berichte der deutschen chemischen Gesellschaft*, 1885, **18**, 439–444.

209   H. Kimura, M. Nakahara and N. Matubayasi, *J Phys Chem A*, 2011, **115**, 14013–14021.

210   V. Tarabanko, M. Smirnova, M. Chernyak, A. Kondrasenko and N. Tarabanko, *Journal of Siberian Federal University. Chemistry*, 2015, **8**, 6–18.

211   S. Meier, A. R. Hansen and P. R. Jensen, *ACS Sustain Chem Eng*, 2023, **11**, 1027–1036.

212   F. Salak Asghari and H. Yoshida, *Ind Eng Chem Res*, 2006, **45**, 2163–2173.

213   B. F. M. Kuster and H. S. van der Baan, *Carbohydr Res*, 1977, **54**, 165–176.

214   B. F. M. Kuster and H. M. G. Temmink, *Carbohydr Res*, 1977, **54**, 185–191.

215   R. Hashaikeh, I. S. Butler and J. A. Kozinski, *Energy & Fuels*, 2006, **20**, 2743–2747.

216   A. Gandini and M. N. Belgacem, *Prog Polym Sci*, 1997, **22**, 1203–1379.

217   G. W. Huber and J. A. Dumesic, *Catal Today*, 2006, **111**, 119–132.

218   H. Rasmussen, H. R. Sørensen and A. S. Meyer, *Carbohydr Res*, 2014, **385**, 45–57.

219   P. S. Divya, S. Nair and S. Kunnikuruvan, *ChemPhysChem*, 2022, **23**, e202200057.

220   H. Shan, L. Li, W. Bai and L. Liu, *ChemistrySelect*, 2022, **7**, e202201237.

221   G. Yang, E. A. Pidko and E. J. M. Hensen, *J Catal*, 2012, **295**, 122–132.

222   J. C. Velasco Calderón, J. S. Arora and S. H. Mushrif, *ACS Omega*, 2022, **7**, 44786–44795.

223   F. J. A. G. Coumans, Z. Overchenko, J. J. Wiesfeld, N. Kosinov, K. Nakajima and E. J. M. Hensen, *ACS Sustain Chem Eng*, 2022, **10**, 3116–3130.

224   S. Constant, H. L. J. Wienk, A. E. Frissen, P. De Peinder, R. Boelens, D. S. van Es, R. J. H. Grisel, B. M. Weckhuysen, W. J. J. Huijgen, R. J. A. Gosselink and P. C. A. Bruijnincx, *Green Chemistry*, 2016, **18**, 2651–2665.

225   K. Cerdan, J. Gandara-Loe, G. Arnauts, V. Vangramberen, A. Ginzburg, R. Ameloot, E. Koos and P. Van Puyvelde, *Soft Matter*, 2023, **19**, 2801–2814.

226   A. Al Ghatta, X. Zhou, G. Casarano, J. D. E. T. Wilton-Ely and J. P. Hallett, *ACS Sustain Chem Eng*, 2021, **9**, 2212–2223.

227   M.-M. Titirici, A. Thomas and M. Antonietti, *New Journal of Chemistry*, 2007, **31**, 787–789.

228   Sironix renewables INC, US10934266B2, 2020.

Green Chemistry Accepted Manuscript

View Article Online

DOI: 10.1039/D4GC06244B

229   C. G. Swain, A. L. Powell, W. A. Sheppard and C. R. Morgan, *J Am Chem Soc*, 1979, **101**, 3576–3583.

230   X. Yue and Y. Queneau, *ChemSusChem*, 2022, **15**, e202102660.

231   R. Demir-Cakan, N. Baccile, M. Antonietti and M.-M. Titirici, *Chemistry of Materials*, 2009, **21**, 484–490.

232   J. Liu, P. Tian, J. Ye, L. Zhou, W. Gong, Y. Lin and G. Ning, *Chem Lett*, 2009, **38**, 948–949.

233   A. Gandini and T. M. Lacerda, *Macromol Mater Eng*, 2022, **307**, 2100902.

234   A. Gandini and M. N. Belgacem, in *Handbook of Thermoset Plastics (Fourth Edition)*, ed. H. Dodiuk, William Andrew Publishing, Boston, 2022, pp. 83–95.

235   WO Pat., WO2018/062995 A1, 2018.

236   Y. Wang, S. Agarwal, A. Kloekhorst and H. J. Heeres, *ChemSusChem*, 2016, **9**, 951–961.

237   R. R. Davda, J. W. Shabaker, G. W. Huber, R. D. Cortright and J. A. Dumesic, *Appl Catal B*, 2005, **56**, 171–186.

238   R. D. Cortright, R. R. Davda and J. A. Dumesic, in *Materials for Sustainable Energy*, Co-Published with Macmillan Publishers Ltd, UK, 2010, pp. 289–292.

239   J. Zakzeski and B. M. Weckhuysen, *ChemSusChem*, 2011, **4**, 369–378.

240   D. Kandemir, P. Van Puyvelde and A. Ginzburg, *ChemSusChem*, 2024, **17**, 1864–5631.

241   T. M. C. Hoang, E. R. H. van Eck, W. P. Bula, J. G. E. Gardeniers, L. Lefferts and K. Seshan, *Green Chemistry*, 2015, **17**, 959–972.

242   T. M. C. Hoang, L. Lefferts and K. Seshan, *ChemSusChem*, 2013, **6**, 1651–1658.

243   Y. Wang, S. Agarwal, Z. Tang and H. J. Heeres, *RSC Adv.*, 2017, **7**, 5136–5147.

244   Y. Wang, S. Agarwal and H. J. Heeres, *ACS Sustain Chem Eng*, 2017, **5**, 469–480.

245   R. M. Abdilla-Santes, S. Agarwal, X. Xi, H. Heeres, P. J. Deuss and H. J. Heeres, *J Anal Appl Pyrolysis*, 2020, **152**, 104963.

246   S. Agarwal, D. van Es and H. J. Heeres, *J Anal Appl Pyrolysis*, 2017, **123**, 134–143.

247   Z. Cheng, B. Saha and D. G. Vlachos, *ChemSusChem*, 2018, **11**, 3609–3617.

248   J. Sun, H. Cheng, Y. Zhang, Y. Zhang, X. Lan, Y. Zhang, Q. Xia and D. Ding, *Journal of Energy Chemistry*, 2021, **53**, 329–339.

249   M. El Fergani, N. Candu, I. Podolean, B. Cojocaru, A. Nicolaev, C. M. Teodorescu, M. Tudorache, V. I. Parvulescu and S. M. Coman, *Catalysts*, 2022, **12**, 1202.

250   F. Stankovikj, A. G. McDonald, G. L. Helms and M. Garcia-Perez, *Energy and Fuels*, 2016, **30**, 6505–6524.

251   J. Feijen, G. van Klink, E. de Jong, A. Schmid, N. Deen and M. Boot, in *SAE Technical Papers*, SAE International, 2017.

252   S. G. Maerten, D. Voß, M. A. Liauw and J. Albert, *ChemistrySelect*, 2017, **2**, 7296–7302.

253   T. Esser, A. Wassenberg, J.-C. Raabe, D. Voß and J. Albert, *ACS Sustain Chem Eng*, 2024, **12**, 543–560.

254   T. Esser, A. Wassenberg, D. Voß and J. Albert, *Chemical Engineering Research and Design*, 2024, **209**, 311–322.

255   S. Kang, G. Zhang, Q. Yang, J. Tu, X. Guo, F. G. F. Qin and Y. Xu, *Bioresources*, 2016, **11**, 9496–9505.

Green Chemistry Accepted Manuscript

256   F. Björnerbäck, D. Bernin and N. Hedin, *ACS Omega*, 2018, **3**, 8537–8545.

257   F. Björnerbäck and N. Hedin, *ACS Sustain Chem Eng*, 2019, **7**, 1018–1027.

258   S. Kang, S. Jiang, Z. Peng, Y. Lu, J. Guo, J. Li, W. Zeng and X. Lin, *Biomass Convers Biorefin*, 2018, **8**, 889–897.

259   G. Yang, H. Chen, H. Qin and Y. Feng, *Appl Surf Sci*, 2014, **293**, 299–305.

260   N. G. Rincón-Silva, J. C. Moreno-Piraján and L. G. Giraldo, *J Chem*, 2015, **2015**, 569403.

261   S. Altenor, B. Carene, E. Emmanuel, J. Lambert, J.-J. Ehrhardt and S. Gaspard, *J Hazard Mater*, 2009, **165**, 1029–1039.

262   L. Li, X. L. Liu, M. Gao, W. Hong, G. Z. Liu, L. Fan, B. Hu, Q. H. Xia, L. Liu, G. W. Song and Z. S. Xu, *J Mater Chem A Mater*, 2014, **2**, 1795–1801.

263   H. Sayğılı and F. Güzel, *J Clean Prod*, 2016, **113**, 995–1004.

264   D. V Chernysheva, Y. A. Chus, V. A. Klushin, T. A. Lastovina, L. S. Pudova, N. V Smirnova, O. A. Kravchenko, V. M. Chernyshev and V. P. Ananikov, *ChemSusChem*, 2018, **11**, 3599–3608.

265   M. Molina-Sabio, M. T. Gonzalez, F. Rodriguez-Reinoso and A. Sepúlveda-Escribano, *Carbon N Y*, 1996, **34**, 505–509.

266   N. Vinod and S. Dutta, *Chemistry (Easton)*, 2023, **5**, 800–812.

267   N. Vinod and S. Dutta, *RSC Adv.*, 2023, **13**, 15141–15147.

268   L. Filiciotto, A. M. Balu, A. A. Romero, E. Rodríguez-Castellón, J. C. Van Der Waal and R. Luque, *Green Chemistry*, 2017, **19**, 4423–4434.

269   L. Filiciotto, P. Tosi, A. M. Balu, E. de Jong, J. C. van der Waal, S. M. Osman, R. Luque and A. Mija, *Molecular Catalysis*, 2022, **526**, 112363.

270   K. Wang, J. Jiang, X. Liang, H. Wu and J. Xu, *ACS Sustain Chem Eng*, 2018, **6**, 15092–15099.

271   J. Yang, X. Niu, H. Wu, H. Zhang, Z. Ao and S. Zhang, *Waste Management*, 2020, **103**, 407–415.

272   R. S. Galaverna, L. P. Fernandes, V. H. Menezes da Silva, A. de Siervo and J. C. Pastre, *European J Org Chem*, 2022, **2022**, e202200376.

273   V. V Karve, T. Schertenleib, J. Espín, O. Trukhina, X. Zhang, M. X. Campins, T. Kitao, C. E. Avalos, T. Uemura and W. L. Queen, *ACS Appl Mater Interfaces*, 2021, **13**, 60027–60034.

274   X. Xiong, I. K. M. Yu, S. Dutta, O. Mašek and D. C. W. Tsang, *Science of The Total Environment*, 2021, **775**, 145851.

275   V. L. Budarin, J. H. Clark, J. Henschen, T. J. Farmer, D. J. Macquarrie, M. Mascal, G. K. Nagaraja and T. H. M. Petchey, *ChemSusChem*, 2015, **8**, 4172–4179.

276   A. Sangregorio, N. Guigo, L. Vincent, E. de Jong and N. Sbirrazzuoli, *Polymers (Basel)*, 2022, **14**, 1019.

277   WO Pat., WO 2018/135941 A1, 2018.

278   R. Dinu, S. Montes, F. Orange and A. Mija, *Compos Sci Technol*, 2021, **207**, 108655.

279   R. Dinu and A. Mija, *J. Mat. Sci. Res.*, 2020, **9**, 29.

280   S. Kang, J. Fu, G. Zhang, W. Zhang, H. Yin and Y. Xu, *Polymers (Basel)*, 2017, **9**, 373.

281   W. Sailer-Kronlachner, C. Rosenfeld, S. Böhmdorfer, M. Bacher, J. Konnerth, T. Rosenau, A. Potthast, A. Geyer and H. W. G. van Herwijnen, *Biomass Convers Biorefin*, 2024, **14**, 8711–8728.

282   J. Vidal, D. Ponce, A. Mija, M. Rymarczyk and P. Castell, *Materials*, 2023, **16**, 1283.

283   EU Pat., EP3728710A1, 2020.

284 A. Ghavidel and R. Hosseinpourpia, *Holzforschung*, 2024, **78**, 283–292.

285 A. Muralidhara, A. Bado-Nilles, G. Marlair, V. Engelen, C. Len and P. Pandard, *Biofuels, Bioproducts and Biorefining*, 2019, **13**, 464–470.

286 A. Gałuszka, Z. Migaszewski and J. Namieśnik, *TrAC Trends Anal. Chem.*, 2013, **50**, 78–84.

287 S. L. Y. Tang, R. L. Smith and M. Poliakoff, *Green Chem.*, 2005, **7**, 761–762.

288 P. T. Anastas and J. B. Zimmerman, *Environ. Sci. Technol.*, 2003, **37**, 94A-101A.

289 R. J. White, N. Brun, V. L. Budarin, J. H. Clark and M.-M. Titirici, *ChemSusChem*, 2014, **7**, 670–689.

290 P. Tosi, G. P. M. van Klink, C. Hurel, C. Lomenech, A. Celzard, V. Fierro, C. Delgado-Sanchez and A. Mija, *Appl Mater Today*, 2020, **20**, 100622.

291 J. Fu, C. Chen, R. L. Jr. Smith and X. Qi, *ACS Sustain Chem Eng*, 2023, **11**, 3832–3840.

292 C. Lomenech, Ch. Hurel, L. Messina, M. Schembri, P. Tosi, F. Orange, F. Georgi, A. Mija and P. Kuzhir, *Waste Biomass Valorization*, 2021, **12**, 6497–6512.

293 Y. Bentahar, C. Lomenech, A. Mija, E. de Jong, E. Bonjour, P. Jame and C. Hurel, *Biomass Convers Biorefin*, 2024, **14**, 13955–13970.

294 A. Sanchez-Sanchez, M. T. Izquierdo, J. Ghanbaja, G. Medjahdi, S. Mathieu, A. Celzard and V. Fierro, *J Power Sources*, 2017, **344**, 15–24.

295 A. G. Pandolfo and A. F. Hollenkamp, *J Power Sources*, 2006, **157**, 11–27.

296 Ö. Gerçel and H. F. Gerçel, *Chem. Eng. J.*, 2007, **132**, 289–297.

297 N. P. Wickramaratne and M. Jaroniec, *ACS Appl Mater Interfaces*, 2013, **5**, 1849–1855.

298 H. A. Patel, J. Byun and C. T. Yavuz, *ChemSusChem*, 2017, **10**, 1303–1317.

299 Q. Ma, K. Fu, J. Zhang, M. Li, X. Han, Z. Chen, L. Ma and C. Chang, *Ind Crops Prod*, 2023, **205**, 117548.

300 W. Hou, S. Wang, X. Ye, Y. Wang and L. Liu, *ACS Sustain Chem Eng*, 2023, **11**, 6129–6135.

301 K. Cerdan, J. Brancart, E. Roels, B. Vanderborght and P. Van Puyvelde, *Polymers*, 2022, **14**, 1657.

302 M. Darder and E. Ruiz-Hitzky, *J Mater Chem*, 2005, **15**, 3913–3918.

303 A. Gómez-Avilés, M. Darder, P. Aranda and E. Ruiz-Hitzky, *Angewandte Chemie International Edition*, 2007, **46**, 923–925.

304 J. F. Leal Silva, E. S. Lopes, A. Chayene Gonçalves, M. R. Wolf Maciel, G. Doubek and R. Maciel Filho, *Chem Eng Trans*, 2022, **92**, 337–342.

305 R. Kalusulingam, S. Gajula, P. Koilraj, D. Shanthana Lakshmi, R. J. Tayade and K. Srinivasan, *ACS Appl Polym Mater*, 2021, **3**, 1932–1942.

306 G. Tzvetkov, M. Nedyalkova, J. Zaharieva, T. Spassov and B. Tsyntsarski, *Powder Technol*, 2019, **355**, 83–92.

307 WO Pat., WO2023/007435A2, 2021.

308 CN Pat., CN 113528084 A, 2021.

309 P. Ares Elejoste, A. Allue, J. Ballestero, S. Neira, J. L. Gómez-Alonso and K. Gondra, *Polymers*, 2022, **14**, 1864.

310 D. Wang and W. Dong, in *Bio-Based Flame-retardant Technology for Polymeric Materials*, eds. Y. Hu, H. Nabipour and X. Wang, Elsevier, 2022, pp. 285–298.

Green Foundation

This review was as carried out using publicly available data from literature, patents, articles and internet as it is indicated in the references list.

Green Chemistry Accepted Manuscript

avantium

P.O. Box 2915, 1000 CX,
Amsterdam, The Netherlands.   +31 20 586 8080

info@avantium.com
www.avantium.com
C of C: 67111386